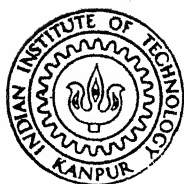


# FABRICATION, ANALYSIS AND PERFORMANCE STUDY OF AN INCLINED SOLAR STILL-CUM-HOT WATER SYSTEM

by

ASHESH KUMAR SINHA

ME TH  
1981 ME/1981/14  
S 64 +  
M  
SIN  
FAB



DEPARTMENT OF MECHANICAL ENGINEERING  
INDIAN INSTITUTE OF TECHNOLOGY KANPUR  
SEPTEMBER, 1981

# **FABRICATION, ANALYSIS AND PERFORMANCE STUDY OF AN INCLINED SOLAR STILL-CUM-HOT WATER SYSTEM**

A Thesis Submitted  
in Partial Fulfilment of the Requirements  
for the Degree of  
**MASTER OF TECHNOLOGY**

by  
**ASHESH KUMAR SINHA**

*to the*

**DEPARTMENT OF MECHANICAL ENGINEERING  
INDIAN INSTITUTE OF TECHNOLOGY KANPUR  
SEPTEMBER, 1981**

ME-1901-M-SIN-FAB

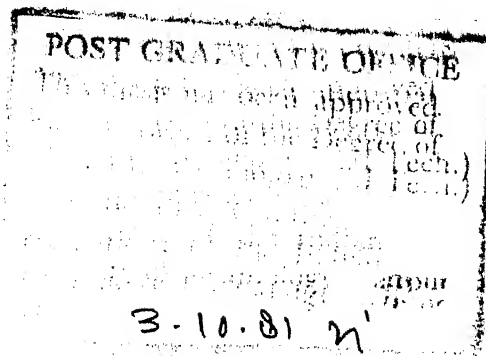
I.I.T. KANPUR  
CENTRAL LIBRARY  
70577  
-5 MAY 1982

25-9-81  
21

## CERTIFICATE

This is to certify that this work on "Fabrication, Analysis and Performance Study of an Inclined Solar Still-cum-Hot Water System" has been carried out under my supervision and it has not been submitted elsewhere for a degree.

*H. C. Agrawal*  
H. C. Agrawal  
Professor and Head  
Department of Mechanical Engineering  
Indian Institute of Technology, Kanpur



#### ACKNOWLEDGEMENT

I wish to express my deep sense of gratitude and sincere regards to Dr. H.C. Agrawal for his constant encouragement and invaluable guidance in the successful completion of this work.

I am also grateful to Dr. P.N. Kaul and Dr. D.P. Rao for their useful suggestions during the course of study.

My sincere thanks are due to Shri S.N. Sharma and Shri Babulal for their constant assistance throughout the period of experimentation. Co-operation rendered by Messers. J.P. Gupta and P.N. Mishra is also gratefully acknowledged.

Lastly, I thank Mr. J.P. Gupta for his excellent typing of the manuscript.

ASHESH KUMAR SINHA

## CONTENTS

	<u>Page</u>
LIST OF TABLES	vi
LIST OF FIGURES	vii
NOMENCLATURE	ix
ABSTRACT	xiv
CHAPTER 1 : INTRODUCTION	1
CHAPTER 2 : THE EXPERIMENTAL SET-UP	10
2.1.1 Description of the Inclined Solar Still	10
2.1.2 The Basin-type Solar Still	14
2.1.3 Pipings, Fittings and Storage Tank	16
2.2 Instrumentation	17
2.2.1 Total Solar Radiation Measurement	17
2.2.2 Temperature Measurement	17
2.2.3 Flow Measurement	19
2.2.4 Wind Velocity Measurement	19
2.3 Modes of Test	20
CHAPTER 3 : HEAT AND MASS TRANSFER ANALYSIS OF THE INCLINED SOLAR STILL	21
3.1 Heat balance of the still	21
3.2 Heat Flux due to Natural Convection	22
3.3 Heat Flux due to Radiation	25
3.4 Heat Flux due to Evaporation and Condensation	26

	<u>Page</u>
3.5      Heat Flux due to Back Losses, from the basin to the surroundings	<b>30</b>
3.6      Heat Flux due to Upward Losses, from the glass cover to the surroundings	<b>31</b>
3.7      Effectiveness of the glass-cover assembly as a heat-exchanger	<b>32</b>
3.8      Still Efficiency	<b>33</b>
CHAPTER 4    :    RESULTS AND DISCUSSIONS	<b>34</b>
4.1      Experimental Procedure	<b>34</b>
4.2      Analysis of the Experimental Data and Results	<b>35</b>
4.3      Conclusions	<b>54</b>
REFERENCES    :	<b>56</b>
APPENDIX 1    :    Evaluation of the Buoyancy Factors for Heat and Mass Transfer in Natural Convection.	<b>58</b>
APPENDIX 2    :    Computer Programme	<b>62</b>

LIST OF TABLES

	<u>Page</u>
Table 4.1(a)      Experimental data obtained for the Inclined Still for the First Mode of Test (top glass cover retained), May 26, 1981.	36
Table 4.1(b)      Results of the test conducted on May 26, 1981.	37
Table 4.2(a)      Experimental data obtained for the Inclined Still for the Second Mode of Test (top glass cover removed), May 27, 1981.	39
Table 4.2(b)      Results of the test conducted on May 27, 1981.	40
Table 4.3           Comparison of daily total yield of distillate for the two types of stills for the month of May, 1981.	43

## LIST OF FIGURES

	<u>Page</u>
Figure 1.1 Schematic Diagram of a Basin-type Solar Still	3
Figure 2.1 Schematic Diagram of the Experimental Set-up.	11
Figure 2.2 Details of the Inclined Solar Still	13
Figure 2.3 Details of the Basin-type Solar Still	15
Figure 2.4 Positions of Thermocouples for the Inclined Solar Still	18
Figure 4.1 Experimental data for the First Mode of Test	44
Figure 4.2 Experimental data for the Second Mode of Test	45
Figure 4.3 Variation of Hourly Yield of disti- llate over the day for the First Mode of Test	46
Figure 4.4 Variation of Hourly Yield of distillate over the day for the Second Mode of Test	47
Figure 4.5 Variation of Cumulative Yield of distillate over the day for the First Mode of Test	48

	<u>Page</u>
Figure 4.6 Variation of Cumulative Yield of distillate over the day for the Second Mode of Test	49
Figure 4.7 Comparison of the Theoretical and Actual Efficiencies of Conversion for the First Mode of Test for the Inclined Still	50
Figure 4.8 Comparison of the Theoretical and Actual Efficiencies of Conversion for the Second Mode of Test for the Inclined Still	51
Figure 4.9 Variation of yield of distillate over Total Insolation for the Inclined Still	52
Figure 4.10 Comparison of daily total yield of distillate for the month of May, 1981	53

## NOMENCLATURE

<u>SYMBOL</u>	<u>DESCRIPTION</u>	<u>UNIT</u>
$A_g$	Area of glass cover	$m^2$
$b$	Thickness of glass-wool insulation	$m$
$c$	Molar concentration of mixture	$Kg\text{-moles}/m^3$
$c_p$	Specific heat at constant pressure	$J/Kgm\text{-}^{\circ}K$
$D_{AB}$	Binary diffusion coefficient of water-vapour in air	$m^2/sec$
$E$	Effectiveness of heat removal	
$F$	Shape factor	
$g$	Acceleration due to gravity	$m/sec^2$
$Gr, Gr_m$	Grashof numbers for heat and mass transfers, respectively	
$h_c$	Convective heat-transfer coefficient, basin-water surface to glass cover	$W/m^2\text{-}^{\circ}K$
$h'_c$	Convective heat-transfer coefficient, top glass cover to ambient	$W/m^2\text{-}^{\circ}K$
$h_D$	Mass-transfer coefficient	$Kgm/m^2\text{-}sec$
$h_{fg}$	Latent heat of condensation	$Kcal/Kgm$
$I_s$	Total insolation on the inclined still	$KJ/m^2\text{-}hr$
$k$	Thermal conductivity	$W/m\text{-}^{\circ}K$
$L$	Distance between the basin-water surface and bottom glass cover	$m$

<u>SYMBOL</u>	<u>DESCRIPTION</u>	<u>UNIT</u>
$m, m_A, m_B$	Masses of the mixture, water-vapour and air, respectively	Kgm
$\dot{m}$	Mass flow rate of saline-water	Kgm/sec
$M_A, M_B$	Molecular weights of water-vapour and air, respectively	Kg/Kg-mole
$N_A$	Molar flux of water-vapour	Kg-moles/m <sup>2</sup> -sec
$N_b$	Yield of distillate from the basin-type still	ml/hr
Nu	Nusselt number	
p	Total pressure of the mixture	Kgf/cm <sup>2</sup>
$p_A, p_B$	Partial pressures of water vapour and air in mixture, respectively	Kgf/cm <sup>2</sup>
Pr	Prandtl number	
$q_a$	Heat flux absorbed by basin-water	W/m <sup>2</sup> -°K
$q_b$	Heat flux due to back losses	W/m <sup>2</sup> -°K
$q_c$	Heat flux due to convection	W/m <sup>2</sup> -°K
$q_e$	Heat flux due to evaporation and condensation	W/m <sup>2</sup> -°K
$q_u$	Heat flux due to upward losses	W/m <sup>2</sup> -°K
$q_r$	Heat flux due to radiation	W/m <sup>2</sup> -°K
Re	Reynold's number	
$R_u$	Universal Gas Constant,	1.9859 $\frac{\text{Kcal}}{\text{Kg-mole-}^{\circ}\text{K}}$

<u>SYMBOL</u>	<u>DESCRIPTION</u>	<u>UNIT</u>
Sc	Schmidt number	
Sh	Sherwood number	
$T, T_a, T_b, T_g$	Temperature at a point, of the ambient, back surface and top glass cover, respectively	°C
$T_{sky}$	Equivalent sky temperature	°C
$T_{w_i}, T_{w_o}$	Inlet and outlet temperatures of the flowing saline water, respectively	°C
$\Delta T$	Temperature difference	°C
$v_{ave}$	Average wind velocity	m/sec
$v, v_A, v_B$	Specific volumes of mixture, water-vapour and air, respectively	$m^3/Kgm$
$V$	Total volume of the mixture	$m^3$
W	Width of the inclined still	m
$\beta_m$	Coefficient of densification	$m^3/Kg\text{-mole}$
$\beta_t$	Coefficient of volume expansion	$1/°C$
$\epsilon, \epsilon_\lambda$	Total and monochromatic emissivities, respectively	
$\epsilon'_g, \epsilon'_W$	Total emissivities of glazing and saline-water, respectively	
$\eta$	Efficiency of conversion of saline-water into fresh water	

<u>SYMBOL</u>	<u>DESCRIPTION</u>	<u>UNIT</u>
$\theta$	Angle of inclination of the still with the horizontal	degrees
$\mu$	Absolute viscosity	$\text{Kgm/m-sec}$
$\rho$	Mass density	$\text{Kgm/m}^3$
$\sigma$	Stefan-Boltzmann constant	$5.67 \times 10^{-8} \text{ W/m}^2 \text{-} \text{K}^4$
$\tau$	Time period	hr

Subscripts

1	refers to the basin-water surface
2	refers to the bottom glass cover
c	calculated
exp	experimental
i	i-th component
lm	logarithmic mean
th	theoretical
z	z-coordinate

## ABSTRACT

An inclined solar still, combining the process of desalination and hot-water production has been developed. Theoretical analysis has been given. Tests have been carried out for a summer month and performance evaluated. The yield of the inclined still has been compared with that of a standard basin-type unit under similar condition.

The essential feature of the solar still developed in the present work consists of a thin film of water flowing continuously over the glass cover, which keeps it cool resulting in high yield of distillate. Heat gained by the water as a result of the heat transfer from the saline water in the basin to the glass cover raises its temperature as it flows over the cover. Thus, hot-water is obtained as a by-product in this process. The entire unit is kept at optimum tilt from the horizontal to receive maximum amount of incoming solar radiation on the basin surface.

A theoretical analysis of the inclined solar still has been carried out and the results compared with those obtained experimentally.

It is concluded that the inclined solar still with cooling-water system is an efficient device for the purpose of desalination. Such units may be installed over large areas near sea-coasts for large-scale production of fresh water.

## CHAPTER - 1

### INTRODUCTION

#### 1.1 WATER SCARCITY, A GLOBAL PROBLEM

Lack of adequate quantities of fresh water has become a serious problem in several countries around the world. Large areas of the earth are arid, due to overwhelming sunshine and lack of rains. In most of these regions, ground water is available, but with a high percentage of mineral content, which makes it unfit for drinking and agricultural purposes. Small villages, situated near sea-coasts, too, face shortage of fresh water during peak periods of summer when fresh-water rivers and lakes nearby become dry, rendering serious drinking water problem to the population. 'Demineralization process' to produce desalinated water from saline or brackish water is not possible to carry out in most of the remote areas, due to non-availability of electricity, necessary for pumping processes and also due to high cost of installation of the demineralization plant.

Thus, in most of these arid zones or regions near a sea, where sunshine is abundant, conversion of saline or brackish water (also available in large quantities) to fresh water by means of solar energy seems to be the only possible solution today.

## 1.2 PRINCIPLE OF SOLAR DESALINATION

The principle of conversion of saline or brackish water to fresh water by means of solar energy can be best understood by referring to the simplest device, designated as the "basin-type solar still." This device is a reproduction, on a very small scale of the hydrologic cycle that occurs in nature, namely, heating of lakes and oceans by the sun's energy causing evaporation, the transport of water-vapour to cooler regions by convective winds and the subsequent condensation of the vapour causing rain and snow. As shown schematically in Fig.1.1, it consists of a blackened basin containing saline water at a shallow depth, over which is an air-tight glass cover that completely encloses the space above the basin. Solar energy, passing through the transparent cover, is absorbed by the water and the basin, warming the water causing evaporation to take place. A temperature difference exists between the hot saline-water surface and the relatively cool glass cover, resulting in convection currents to set up in the air, trapped inside the enclosure. These currents bring the humid air in contact with the glass cover, causing condensation of the vapour on the underside of the cover. The condensate slides down the slope, flows along the distillate channel and is collected in a container.

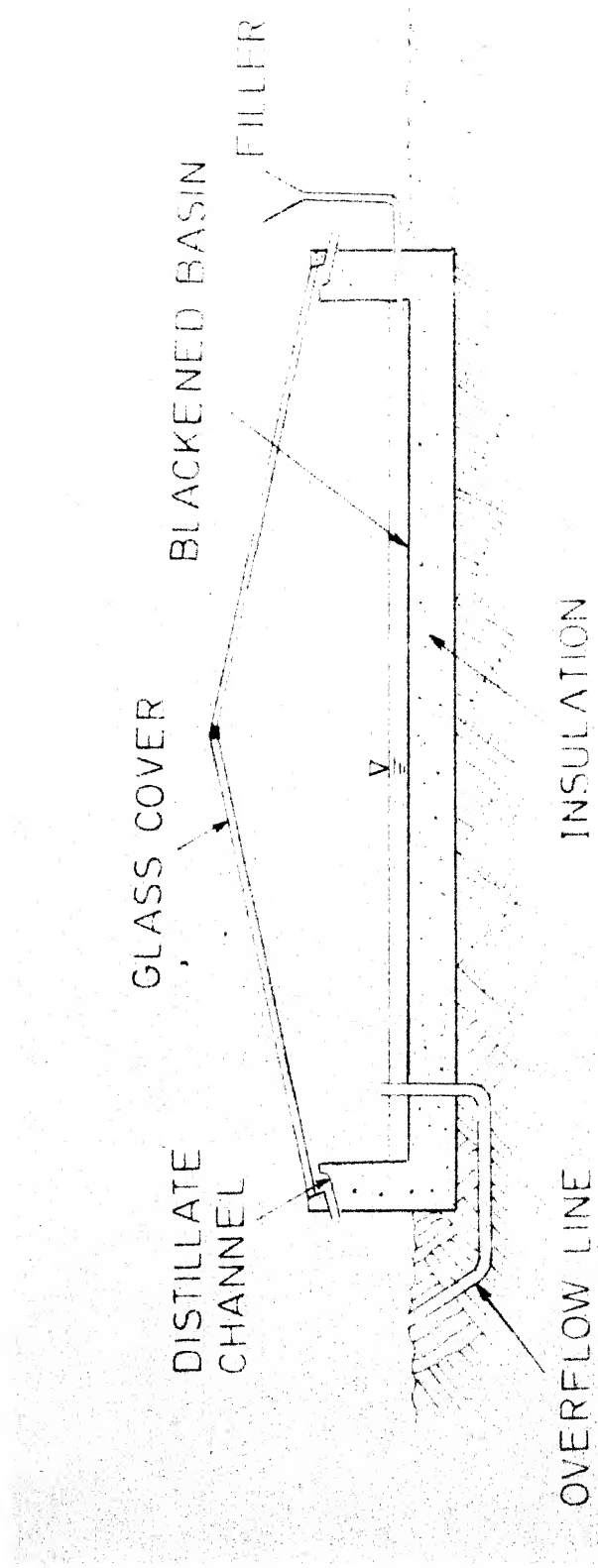


FIG. 1.1 SCHEMATIC DIAGRAM OF A BASIN-TYPE SOLAR STILL

### 1.3 ADVANTAGES OF SOLAR DESALINATION

Some of the important factors favouring solar desalination are as following :

- (1) In arid regions where there is no other source to obtain drinking water, solar desalination is the only solution.
- (2) Solar energy is used as a substitute for fuel in solar desalination process to heat the saline water to form vapours which later condense to produce fresh water. In view of the present scarcity and high cost of fuels like coal, oil and gas all over the world, use of solar energy, which is free, inexhaustible and non-polluting in nature, is an attractive idea for desalination purpose.
- (3) Solar desalination is most effective during the peak periods of sunshine, when the demand for fresh-water is also very high. Also, during rainy season, when solar stills are not very effective, they can be used to collect rain water as fresh water. Thus, the demand and supply are effectively geared in this desalination process.
- (4) Unlike the problem of installation of flat-plate collectors in populated areas where space problem is acute, solar stills in most cases, are installed

over vast areas in the arid region, which are otherwise lying barren. Production of fresh water in these arid zones may facilitate in utilizing large areas of land in future.

#### 1.4 REVIEW OF PREVIOUS WORK

Historically, instances of application of solar energy to fresh water production have been recorded throughout the world and at various times during the past century. The unit which has been built and used extensively in the past and is still the most popular device for desalination purpose today, is the simple basin-type solar still, already discussed. The largest basin-type solar still was built in the year 1872 near Las Salinas in northern Chile. This unit had a basin area of  $4700 \text{ m}^2$  and it produced 22700 litres of pure water per day to the needs of a nitrate mining community for many years.

During the World War II and the decade immediately following, sustained drought conditions in many parts of the world brought water supply into sharp focus. This resulted in the development of inflated plastic stills by Maria Telkes<sup>1</sup>. The unit consisted of an inflatable plastic-envelope containing a felt-pad which was to be saturated with sea-water. Solar energy, striking the felt-pad, would produce vapour which would condense on the inside of the plastic-envelope and drip into the bottle at the bottom of

the assembly. Although, plastic stills are relatively cheap, their yield is low due to the formation of drop-wise condensation under the plastic roof, causing high reflection losses of incoming solar radiation. The efficiency of such stills, is less than 40 percent.

Tilted solar stills using porous pads as evaporating surfaces have also been used widely for many years. The upper end of the pad is immersed in a trough containing salt water, which spreads over the cotton by capillary action. Evaporation and condensation take place as usual. Although, the unit is cheap and easy to fabricate, yield is quite low due to low temperature of the evaporating surface. A maximum efficiency of 50 per cent has been reported for such stills.

A solar still with a low thermal inertia has been developed by Szulmayer<sup>2</sup>. It is essentially a basin-type still with a floating, black absorber sheet to heat a thin layer of water (1.6 - 6.3 mm thick) on the top of the sheet, causing rapid evaporation. Since the base of the still is kept cooler, heat loss through conduction to the ground is reduced. The rate of evaporation (using a woven black shade cloth as the floating absorber) has been reported to be 0.308 litres/m<sup>2</sup>-hr.

Efforts have been made to increase the temperature of the basin-water by means of concentrating devices. A 'mini solar-still' designed by Muthuveerappan, et al.<sup>3</sup>,

incorporates mirror-type reflectors to concentrate solar energy on the tray. A 50-60 per cent increase in the yield of distilled water and a mean efficiency of 56 per cent have been reported. However, the extra cost of reflectors seems to outweigh the effect of increase in the yield.

Lobo, et al.<sup>4</sup> have tested a multi-effect, basin-type solar still, which uses the upward heat fluxes due to convection, radiation and evaporation to heat a secondary basin consisting of an inclined-stepped glass tray. The upward heat-fluxes from the secondary basin are used to heat water contained in a third basin, similar in construction to the previous one. The condensate from each effect is collected in separate bottles. Although, an increase in yield of 40 - 50 per cent over the standard basin-type unit has been reported, the unit suffers from constructional difficulties, leakages of both saline-water and water-vapour through the linings and lack of long-term durability.

A second type of regenerative unit has been developed by Akhtamov, et al.<sup>5</sup>. This unit incorporates the reuse of upward heat fluxes to heat a layer of saline-water which is enclosed between two glass-covers and flows upwards due to hydrostatic pressure exerted by the saline-water contained in an overhead tank. The saline-water absorbs heat and is allowed to be fed into the basin to compensate for the evaporation of saline water. This process results in the preheating of the saline feed-water to the basin. An

efficiency of 60 per cent has been reported by the authors. However, since the rate of discharge of hot saline water to the basin is very small, the problem of cooling the cover assembly to obtain higher yield yet remains to be solved.

In view of the large area required to produce a given quantity of water by means of the basin-type stills, investigators have tried vertical type, multi-effect solar stills. One such unit developed by Dunkle<sup>6</sup> consists of vertical parallel plates within an enclosure in which hot saline water is made to flow down the surface of a plate causing evaporation. Condensation take place along the surface of an adjacent vertical plate, which is kept cool by allowing cold saline water to run down along the other surface of it. A series of such evaporators and condensers are installed to obtain higher yield. However, this increase in distiller performance is yet to be justified in terms of the large capital cost on the total plant economy.

### 1.5 THE PRESENT WORK

In most of the work on solar desalination, as reviewed above, the conversion efficiency has not been more than 60 per cent. The present effort is directed towards developing a more efficient still which acts as an auxiliary hot-water device as well. The main feature of the solar still developed in the present work consists of a box-type unit in which a thin film of water flows

continuously over the glass cover and keeps it cool, resulting in high yield of distillate. The saline water is stored in an overhead tank and fed continuously to the still through a perforated tube. Upward heat fluxes due to convection, radiation and evaporation get transferred to the thin film of water, whose temperature increases as it flows along the glass. Thus, in addition to high output of desalinated water due to increased evaporation rate, hot water, also, is obtained continuously throughout the day, which may be either stored or used to heat some auxiliary devices. The entire unit is kept at optimum tilt from the horizontal to receive the maximum amount of incoming solar radiation on the basin surface.

Chapter-2 describes the design and fabrication details of both the inclined and the basin-type stills for a comparative study. It also describes the instrumentation involved in the experiments and the modes of tests conducted.

In Chapter-3, heat and mass transfer analysis of the inclined still has been carried out.

The results obtained both from theoretical analysis and experiments carried out are discussed in Chapter-4. The hourly and cumulative yields of the inclined still are compared with that of the standard single roof, basin-type unit for a summer month.

## CHAPTER - 2

### THE EXPERIMENTAL SET-UP

The experimental set-up that was used for testing the performance of the inclined solar still and for comparing it with the basin-type unit is shown in Fig. 2.1.

#### 2.1.1 DESCRIPTION OF THE INCLINED SOLAR STILL

The constructional details of various important parts of the inclined solar still are shown in Fig. 2.2 and discussed below.

The saline-water basin consists of 60 cms long aluminium angles (1cm x 1cm, 0.5 mm thick) placed in adjacent rows and fixed to the bottom of a rectangular box (60cms x 60cms x 10.6 cms) made of 22 gauge (0.85344 mm mean thickness) G.I. sheet. The channelled basin, thus, can contain about 3.6 litres of saline water when filled to a depth of 1 cm. To prevent leakage of water from one channel to the other through the sides, a rubber gasket, 1 mm thick, surrounds the periphery of the basin. The basin is painted with black paint mixed with black mesh powder, and later made dull by rubbing with emery paper to make it a good solar energy absorber.

### NOMENCLATURE

① BASIN-TYPE SOLAR STILL  
② INCLINED SOLAR STILL  
③ INLET FOR SALINE WATER TO BASIN  
④ INLET FOR SALINE WATER TO COOL  
THE BOTTOM GLASS COVER  
⑤ HOT SALINE WATER OUTLET  
⑥ CONDENSATE DRAIN  
⑦ BASIN OVERFLOW AND DRAIN  
⑧ PLASTIC BOTTLE (500ML) TO  
COLLECT THE CONDENSATE  
⑨ TROUGH FOR COLLECTING  
SALINE WATER  
⑩ SALINE WATER OUTLET FROM  
TROUGH TO DRAIN

⑪ 5.5MM WINDOW GLASS  
⑫ SALINE WATER BASIN  
⑬ GLASS WOOL INSULATION  
⑭ SALINE WATER STORAGE  
TANK

⑮ OVERFLOW FOR TANK  
⑯ GRADUATED WATER-  
LEVEL INDICATOR  
⑰ STEEL FRAME-WORK  
⑲ HINGED JOINT TO ADJUST  
THE ANGLE OF TILT OF  
THE STILL

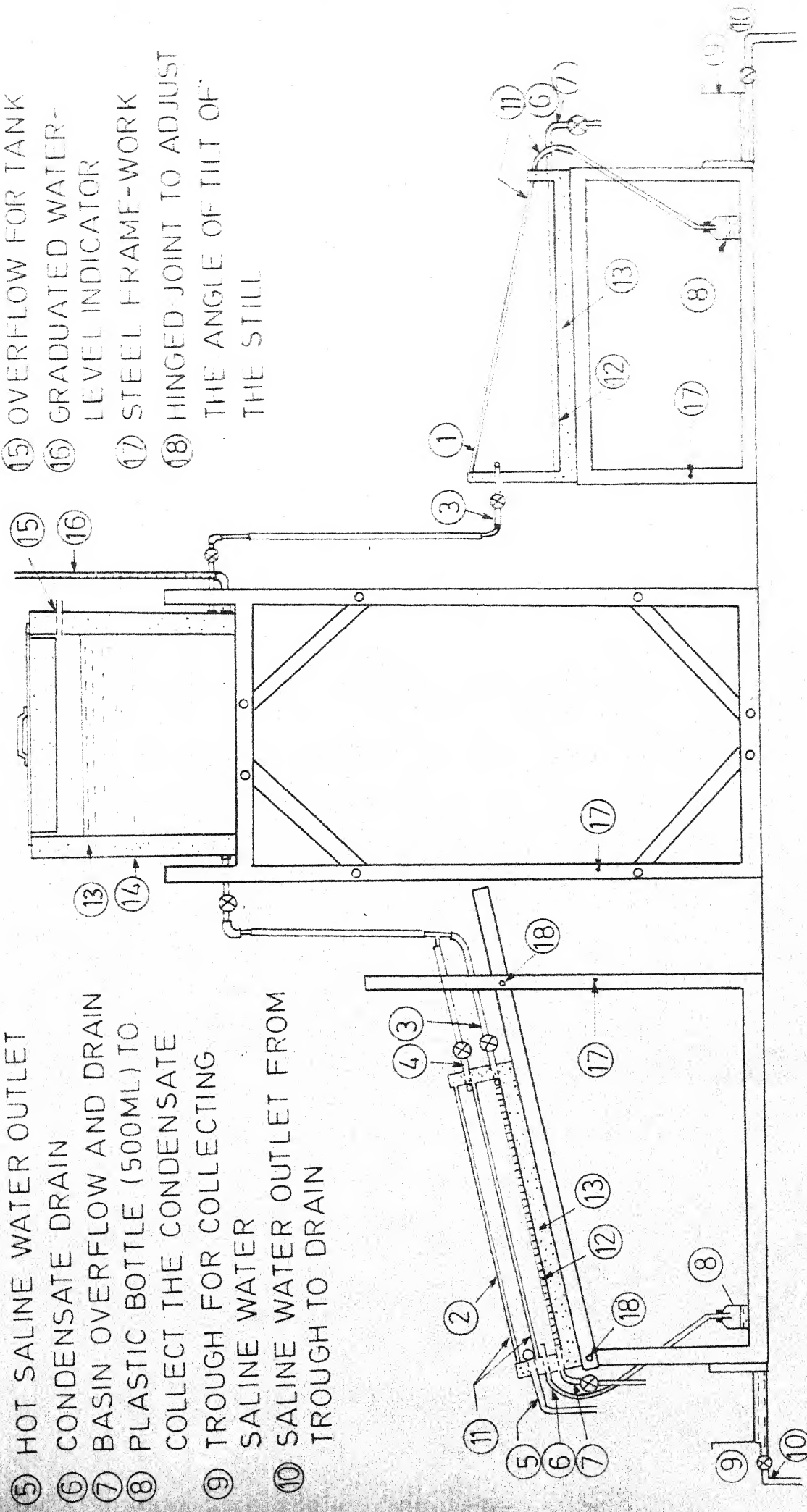


FIG.21 SCHEMATIC DIAGRAM OF THE EXPERIMENTAL SET-UP

Common window glass (60cms x 60cms, 5.5 mm thick) is used for the top covers of the still. Glass transmits incoming solar radiation in the range of 0.3 to 3.0 microns, but is opaque to radiation emitted by the hot absorber plate and the water surface, beyond 4.8 microns. Hence, the still serves as a hot-box. The glass cover rests on aluminium angles, fixed along the periphery of the box. It is sealed to the box by means of rubber gaskets and adhesive along its four sides to make it air-tight, so that no water-vapours may leak outside through the edges. A gap of 5 cms is maintained between the basin water surface and the glass cover. This distance of 5 cms was chosen to reduce the shading of the basin water surface by the lateral walls of the solar still and also to decrease the fabrication cost. The top glass cover, similarly, rests lightly on aluminium angles, provided with rubber gaskets, along the periphery of the box, but it is removable. The top glass cover is periodically treated with dilute hydrochloric acid to remove the formation of dust coatings.

To prevent heat losses from the bottom and sides of the still, the unit is enclosed in a rectangular box (64cms x 64cms x 16.6cms) made of 22 gauge G.I. sheet, and the space in between is filled with 6 cms thick glass wool at the bottom and 2 cms thick on the sides.

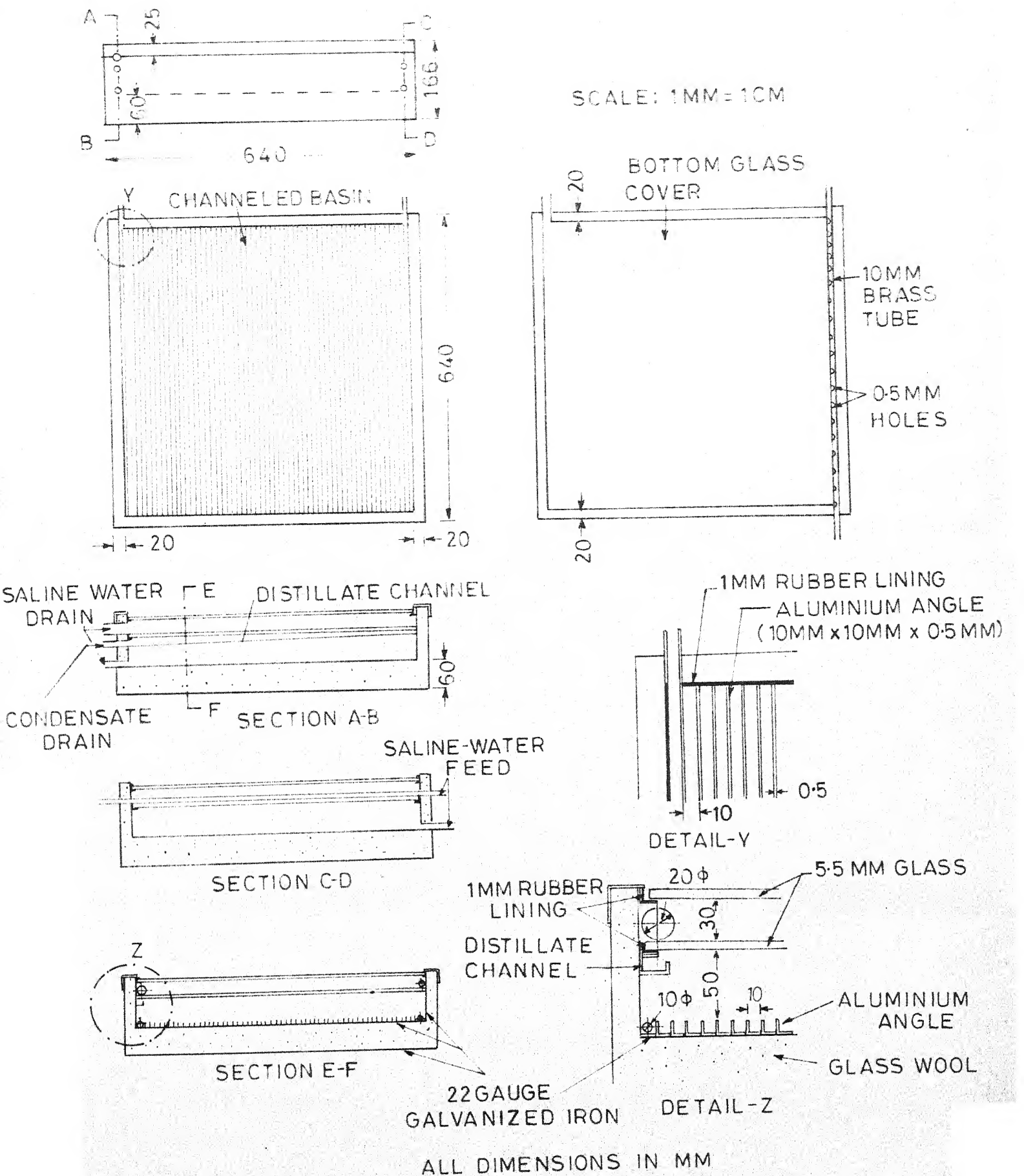


FIG. 2.2 DETAILS OF THE INCLINED SOLAR STILL

### 2.1.2 THE BASIN-TYPE SOLAR STILL

The constructional details of the basin-type still are shown in Fig. 2.3.

It consists of a box with base dimensions of 60cms x 60 cms, front and rear wall heights of 6 cms and 18.5 cms, respectively. The still has an inclined roof on which rests a 5.5 mm thick glass cover, sloping at an angle of  $12^{\circ}$  with the horizontal to prevent the condensate from dropping into the basin. The glass cover rests on rubber linings and is secured properly in its place by means of aluminium angles, fixed with screws along the periphery of the still. The condensate slides down the slope of the glass cover, flows in a U-shaped channel from where it is collected in a plastic bottle. Saline water is filled upto a small depth (about 1 cm) in the basin for maintaining a low thermal inertia. The basin surface is painted with black paint mixed with black mesh powder for better absorption of solar radiation.

The basin-type still is also enclosed in a box with base dimensions of 64cms x 64cms, front and rear wall heights of 12 cms and 24.5 cms, respectively. Both the inner and the outer boxes are made of 22 gauge G.I. sheet and the space in between is filled with 6 cms thick glass wool at the bottom and 2 cms thick on the sides to prevent heat losses to the surroundings.

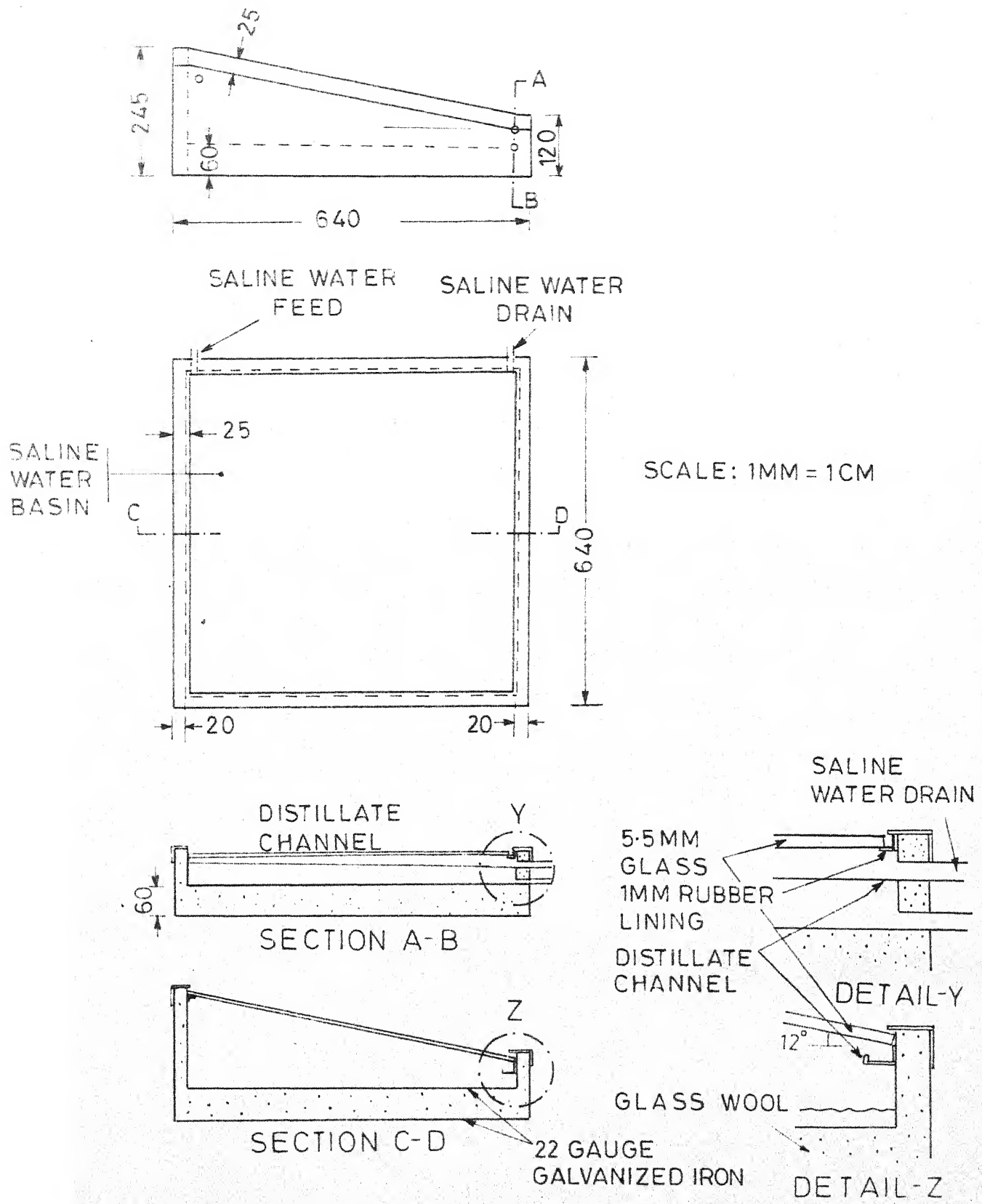


FIG.23 DETAILS OF THE BASIN-TYPE SOLAR STILL

### 2.1.3 PIPINGS, FITTINGS AND STORAGE TANK

The arrangement of the pipings, valves and other connections for both the stills is shown in Fig. 2.1. Polythene pipes with plastic valves and connections have been used for ease of installation and low cost, as well. For the inclined still, the condensate is collected in a U-shaped channel, running along the underside of the glass cover at its edge as shown in Fig. 2.2. Also, a 1 cm dia. brass tube with uniformly spaced holes of 2 mm dia. drilled along its length is used to feed the cold saline water to flow over the glass plate. The hot-water obtained as a by-product, flows out through the exit pipe into a trough placed on the ground, from where it is drained away.

A storage tank of capacity 200 litres, is provided to feed the saline water to both the stills. It has two separate valves connected to the outlet pipes of the tank, providing saline water to each basin and cold saline water to cool the bottom glass cover of the inclined still. A graduated water-level indicator made of glass is fitted to the storage tank. The tank is insulated with 6 cms thick glass-wool along its sides to prevent the stored saline-water from being heated up.

## 2.2 INSTRUMENTATION

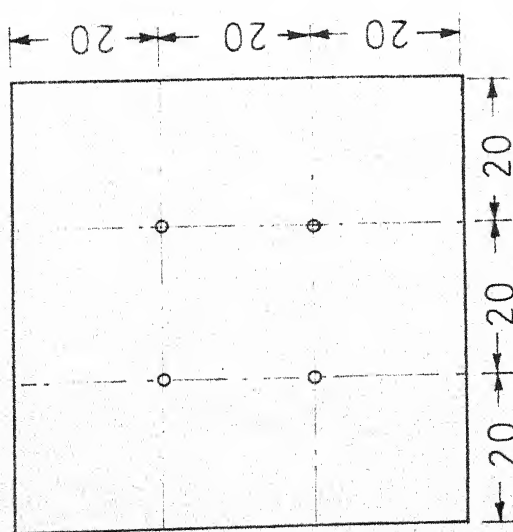
### 2.2.1 TOTAL SOLAR RADIATION MEASUREMENT

The total radiation incident on the basin of the inclined still consists of both the direct and diffuse radiation. An Eppley Pyranometer has been used to measure the total radiation falling on the inclined surface. The instrument was kept facing south and tilted at the angle of inclination of the still, and the output recorded on an hourly interval by the Eppley Integrator.

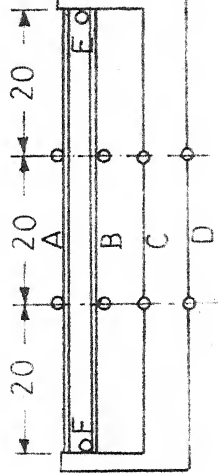
### 2.2.2 TEMPERATURE MEASUREMENT

All temperatures, except the ambient have been measured by 24 gauge, calibrated copper-constantan, insulated thermocouples, and the output recorded directly on the graph paper by a 24-junction Honey-well Temperature Recorder, having a least count of  $1^{\circ}\text{C}$ . Fig. 2.4 shows the positions of the thermocouples on the inclined still. The top glass cover has four thermocouples fixed to its upper surface by adhesive as shown. Similarly, four thermocouples have been fixed to the underside of the bottom glass cover to measure the average temperature of the condensate film. Four thermocouple wires have been soldered to the channelled basin and four to the bottom surface of the still. Two thermocouples, each immersed in the flowing water film were used to measure the inlet and outlet temperatures of the water film. Ambient temperature was measured by a mercury-in-glass thermometer with a least count of  $1^{\circ}\text{C}$ , placed in shade.

POSITION OF THERMOCOUPLES	NUMBER	TEMPERATURE
A	4	$T_g$
B	4	$T_2$
C	4	$T_1$
D	1	$T_b$
E	1	$T_{wi}$
F		$T_{wo}$



TOP VIEW



SIDE VIEW

ALL DIMENSIONS IN MM

FIG.24 POSITIONS OF THERMOCOUPLES FOR THE  
INCLINED SOLAR STILL

### 2.2.3 FLOW MEASUREMENT

A graduated, water-level indicator made of glass, fitted to the storage tank, as shown in Fig.2.1, is used to note the decrease in the level of saline water over an hourly interval of time. Knowing the area of cross-section of the tank, the mass flow rate of saline water can be found out.

The condensate collected in plastic bottles was measured on an hourly basis by means of a graduated cylinder of 500 ml capacity, having a least count of 5 ml.

### 2.2.4 WIND VELOCITY MEASUREMENT

Due to non-availability of a windscope, the velocity of wind was measured by means of a rotating, vane-type anemometer, which was adjusted every time to take into account the change in the direction of the wind velocity.

### 2.3 MODES OF TEST

The performance of the inclined still was tested under two modes of operations.

In the first mode, the top glass cover (which is removable) was placed over the still to prevent cooling of the film of flowing water due to its surface being exposed to the ambient, thus retaining the hot water which often reached more than 48 °C during the peak hours of sunshine. This arrangement, however, decreased the amount of incoming radiation due to the addition of the top glass cover, resulting in lower yield.

The second mode of test was conducted with the top glass cover removed. In this case, yield of distillate was more, but the temperature of the hot water was substantially reduced due to the rapid heat loss from the water film to the ambient.

## CHAPTER - 3

### HEAT AND MASS TRANSFER ANALYSIS OF THE INCLINED SOLAR STILL

#### 3.1 HEAT BALANCE OF THE STILL

Assuming steady-state operation of the still, the following equations can be written :

Heat balance for basin water :

$$q_a = q_c + q_r + q_e + q_b \quad (3.1)$$

Heat balance for the bottom glass cover :

$$q_c + q_r + q_e = \frac{\dot{m}}{A_g} c_p (T_{w_o} - T_{w_i}) + q_b \quad (3.2)$$

where,

- $q_a$  - incident solar energy flux absorbed by the basin-water,
- $q_c$  - heat flux due to natural convection from the basin-water surface to the glass cover,
- $q_r$  - heat flux due to radiation from the basin-water surface to the glass cover,
- $q_e$  - heat flux due to evaporation and condensation from the basin-water to the glass cover,

$q_b$  - heat flux due to back losses from the basin  
 to the surroundings,  
 $q_g$  - heat flux due to upward losses from the glass  
 cover to the surroundings,  
 $m$  - mass flow rate of saline water over the glass  
 cover,  
 $A_g$  - area of the glass cover,  
 $T_{w_i}, T_{w_o}$  - inlet and outlet temperatures of the saline  
 water flowing over the glass cover,  
 respectively.

The various heat fluxes are evaluated in the following sections :

### 3.2 HEAT FLUX DUE TO NATURAL CONVECTION

The process of heat transfer inside the still is due to natural convection arising as a result of the density difference of the fluid enclosed between the two parallel surfaces, the basin surface at temperature  $T_1$  and the glass surface at temperature  $T_2$ , where  $T_1 > T_2$ . Under such circumstances, the heat transfer coefficient is obtained from the empirical relation<sup>7</sup>,

$$Nu = [2.44 + \{2.23 - 0.01230 + 0.00034\theta^2\} \left\{ \left( \frac{Gr \Pr \cos\theta}{Ra_t} \right)^{1/3} - 1 \right\}]$$

valid for  $10 < Gr \Pr < 4 \times 10^6$   
 $0^\circ < \theta < 60^\circ$  (3.3)

where,

$Nu$  = Nusselt number

$$= \frac{h_c L}{k}$$

$Gr$  = Grashof number for heat transfer

$$= \frac{g L^3 \rho^2 \beta_t (T_1 - T_2)}{\mu^2}$$

$Pr$  = Prandtl number

$$= \frac{\mu c_p}{k}$$

$$Ra_t = 11300[1 + 0.204 \sin 4.50(\theta - 37.8^\circ)]$$

$\theta$  = Angle of inclination of the still with the horizontal

$L$  = Distance between the two surfaces at temperatures  $T_1$  and  $T_2$ , respectively

$g$  = Acceleration due to gravity

$\beta_t$  = Coefficient of volume-expansion of the air-water vapour mixture in the still

$h_c$  = Convective heat-transfer coefficient

$\rho$ ,  $\mu$ ,  $c_p$ , and  $k$  denote the density, viscosity, specific heat and thermal conductivity of the mixture in the still.

The term  $\beta_t(T_1 - T_2)$ , known as the 'buoyancy factor' for heat transfer was originally evaluated for conditions of constant

composition of the convecting fluid, and was given by

$$\beta_t (T_1 - T_2) = \frac{T_1 - T_2}{(T_1 + T_2)/2}$$

However, in the still, the humidity of the air and, therefore, its composition changes along the flow path. The vapour formed in the still is lighter than the dry air component and therefore, increases the buoyant force and the rate of circulation of the air and associated vapour. The modified expression for the buoyancy factor as derived in Appendix-1 is given by

$$\beta_t (T_1 - T_2) = \frac{T_1 - T_2}{T_2} + \left[ \frac{\frac{p_{A_1} - p_{A_2}}{M_B} - p}{\left( \frac{M_B - M_A}{M_B} \right) p - p_{A_1}} \right] \frac{T_1}{T_2} \quad (3.4)$$

where,

$p_{A_1}$  = partial pressure of saturated water-vapour at temperature  $T_1$ .

$p_{A_2}$  = partial pressure of saturated water-vapour at temperature  $T_2$ .

$p$  = total pressure inside the still (assumed at 1 atmosphere).

$M_A$  = Molecular weight of water-vapour.

$M_B$  = Molecular weight of dry air.

The expression (3.4) is used to determine the Grashof number occurring in expression (3.3).

The heat flux due to convection is given by

$$q_c = h_c (T_1 - T_2)$$

where, the heat transfer coefficient is evaluated from equation (3.3).

### 3.3 HEAT FLUX DUE TO RADIATION

The heat transfer due to radiation can be approximated as taking place between two parallel surfaces of equal areas enclosing a non-absorbing, non-emitting medium. The radiation involved is diffuse radiation in the long wavelength range, for which the glass and water can be treated as grey surfaces ( $\epsilon_\lambda = \epsilon$ ). Under such circumstances, the heat transfer due to radiation is expressed as

$$q_r = F \sigma (T_1^4 - T_2^4)$$

where,

$\sigma$  = Stefan-Boltzmann constant

$$= 5.67 \times 10^{-8} \frac{\text{Watts}}{\text{m}^2 \text{ - } ^\circ\text{K}^4}$$

$F$  = Shape factor

$$= \frac{1}{\frac{1}{\epsilon_w} + \frac{1}{\epsilon_g} - 1}$$

$\epsilon_w$  = emissivity of the saline-water in the basin.

$\epsilon_g$  = emissivity of the water film-glass glazing.

Taking the emissivities of saline-water and glazing as 0.96 and 0.95, respectively, we obtain  $F = 0.9$ . Hence,

$$q_r = 0.9 \sigma (T_1^4 - T_2^4) \quad (3.5)$$

### 3.4 HEAT FLUX DUE TO EVAPORATION AND CONDENSATION

In addition to convection and radiation, the bulk of the heat transferred upwards is due to evaporation of water from the basin surface and its subsequent condensation on the glass cover. The evaluation of the heat transfer due to evaporation and condensation is carried out in three steps, namely, evaluation of

(i) mass-transfer coefficient,

(ii) rate of mass-transfer,

and (iii) heat flux due to evaporation and condensation.

(i) Evaluation of the mass-transfer coefficient :

The process of heat transfer due to natural convection inside the still is accompanied by mass-transfer due to evaporation of water from the basin. For the case of simultaneous heat and mass transfer inside a fixed geometry and in the absence of any chemical reaction, it may be shown that the

governing equations and the boundary conditions for heat and mass transfer processes are similar and hence, they can be treated as analogous in nature<sup>8</sup>. The solution of heat transfer problem in case of natural convection can be written in terms of dimensionless quantities as follows:

$$Nu = f(Gr, Pr)$$

Since the heat and mass transfer processes are analogous, the solution of mass-transfer problem can be written as

$$Sh = f(Gr_m, Sc)$$

where, the functional relationships are the same<sup>9</sup>.

The dimensionless quantities in the above equations are:

Sh = Sherwood number

$$= \frac{h_D L}{\rho D_{AB}}$$

Sc = Schmidt number

$$= \frac{\mu}{\rho D_{AB}}$$

and  $Gr_m$  = Grashof number for mass-transfer

$$= \frac{g L^3 \rho^2 \beta_m (c_1 - c_2)}{\mu^2}$$

where,  $h_D$  and  $D_{AB}$  denote the mass-transfer coefficient and diffusion coefficient, respectively, of water-vapour in air.

$c_1$  and  $c_2$  denote the concentrations of air water-vapour mixture at the lower and upper surfaces of the still, respectively.

$\beta_m$  is known as the coefficient of densification which indicates the variation of density with composition for mass-transfer.

The term  $\beta_m(c_1 - c_2)$  is evaluated in a similar manner as the term  $\beta_t(T_1 - T_2)$  [See Appendix-1] and is given by

$$\beta_m(c_1 - c_2) = \frac{T_1 - T_2}{T_1} + \left[ \frac{\frac{p_{A_1} - p_{A_2}}{M_B}}{\left( \frac{M_B - M_A}{M_B} \right) p - p_{A_2}} \right] \frac{T_2}{T_1} \quad (3.6)$$

The expression (3.6) is used to determine the value of  $Gr_m$ . Hence, in equation (3.3), after replacing  $Nu$  by  $Sh$ ,  $Gr$  by  $Gr_m$  and  $Pr$  by  $Sc$  and solving for the mass transfer coefficient, we get,

$$h_D = \frac{\rho_{AB}^D}{L} [ 2.44 + \left\{ 2.23 - 0.0123\theta + 0.00034\theta^2 \right\} \left\{ \left( \frac{Gr_m \cdot Sc \cdot \cos\theta}{Ra_t} \right)^{1/3} - 1 \right\} ] \quad (3.7)$$

### (ii) Evaluation of the rate of mass-transfer

Let the two components of the gaseous mixture inside the still, consisting of water vapour and air be denoted by A and B, respectively. The molar flux of component A in the  $z$  - direction is given by <sup>10,11</sup>

$$N_{Az} = h_D \frac{p_{A_1} - p_{A_2}}{p_{B_{lm}}} \quad (3.8)$$

where  $p_{Blm}$  = log-mean pressure of component B

T = mean temperature of the mixture

$R_u$  = Universal Gas Constant

For normal air, water-vapour mixture at atmospheric pressure, the partial pressure of one component does not vary significantly in comparison to the total pressure<sup>12</sup>. Hence,

$$p_{Blm} \approx \frac{p_{B1} + p_{B2}}{2}$$

From Dalton's Law of partial pressure,

$$p_A + p_B = p$$

Therefore,

$$\begin{aligned} p_{Blm} &= \frac{(p - p_{A1}) + (p - p_{A2})}{2} \\ &= \left( \frac{2p - p_{A1} - p_{A2}}{2} \right) \end{aligned} \quad (3.9)$$

Substituting the value of  $p_{Blm}$  in Eqn. (3.8) and denoting  $N_{Az}$  by N, we obtain,

$$N = h_D \frac{p}{R_u T} \frac{(p_{A1} - p_{A2})}{(2p - p_{A1} - p_{A2})/2} \quad (3.10)$$

Thus,  $N$  denotes the mass-transfer rate of water-vapour due to evaporation. The value of  $h_D$  is obtained from Eqn. (3.7). The properties of the mixture are evaluated<sup>13,14</sup> at the mean temperature,  $(T_1 + T_2)/2$ .

(iii) Heat Flux due to evaporation and condensation :

The heat flux due to evaporation and condensation is given by

$$q_e = N h_{fg}$$

where,  $h_{fg}$  denotes the latent heat of condensation evaluated<sup>14</sup> at the glass temperature  $T_2$ .

A computer programme to evaluate the mass-transfer rate alongwith the upward heat fluxes due to convection, radiation and evaporation is included in Appendix-2.

### 3.5 HEAT FLUX DUE TO BACK LOSSES FROM THE BASIN TO THE SURROUNDINGS

The heat transfer due to back losses is given by,

$$q_b = \frac{k}{b} (T_1 - T_b)$$

where,  $k$  = thermal conductivity of the glass wool insulation,  
 $b$  = thickness of glass-wool insulation at the bottom,  
 $T_b$  = temperature of the back surface of the still.

### 3.6 HEAT FLUX DUE TO UPWARD LOSSES FROM THE GLASS COVER TO THE SURROUNDINGS

The rate of heat dissipation depends both on radiation to the sky and on convection by air circulation. Radiation to the sky depends on the equivalent sky temperature,  $T_{sky}^*$ . The convective portion, is taken as a function of wind velocity. The total heat flux is given by

$$q_x = \varepsilon_g \sigma [ T_g^4 - (T_a - ll)^4 ] + h_c' (T_g - T_a)$$

where,

$T_g$  = temperature of the top glass cover,

$T_a$  = temperature of the ambient,

$\varepsilon_g$  = total emissivity of glass (taken as 0.95),

\* The sky can be considered as blackbody at some equivalent sky temperature, which accounts for the fact that the atmosphere is not at a uniform temperature. Among the several expressions proposed for evaluating the sky temperature, the one which is most commonly used is given by

$$T_{sky} = T_a - ll,$$

where,  $T_{sky}$  and  $T_a$  denote the sky temperature and ambient temperature in  $^{\circ}\text{C}$ , respectively.

$\sigma$  = Stefan-Boltzmann constant

$$= 5.67 \times 10^{-8} \frac{\text{Watts}}{\text{m}^2 \text{-} \text{oK}^4}$$

$h'_c$  = outside convective heat-transfer coefficient,  
and is given by <sup>15</sup>

$$\frac{h'_c \text{ W}}{k} = 0.028 \text{ Re}^{0.8}$$

where, W = width of the still, and

$\text{Re}$  = Reynold's number

$$= \frac{\rho v_{\text{ave}} W}{\mu}$$

$v_{\text{ave}}$  = Average wind velocity.

$\rho$ ,  $\mu$  and  $k$  denote the density, viscosity and thermal conductivity of the air, evaluated <sup>13</sup> at the film temperature,  $(\frac{T_g + T_a}{2})$ .

The heat flux,  $q$ , obtained experimentally, as shown above, is compared with the value calculated from Eqn. (3.2) and the results shown in column 8 of Table 4.1(b).

### 3.6 EFFECTIVENESS OF THE GLASS-COVER ASSEMBLY AS A HEAT EXCHANGER

The glass-cover assembly serves as a heat exchanger in which heat transfer takes place between the water-film enclosed by the cover assembly and the upward heat fluxes due to convection, radiation and evaporation. Neglecting the

small amount of heat transfer in the inlet pipes, the saline water enters at the outlet temperature of the water in the tank, and leaves at a considerably higher temperature due to the heat gained, as it flows over the glass surface. The effectiveness,  $E$  of the cover-assembly as a heat exchanger can be defined as the ratio of the actual quantity of heat removed by the flowing water to the maximum possible heat transferred to the water. i.e.

$$E = \frac{\frac{\dot{m}}{A} c_p (T_{w_o} - T_{w_i})}{q_c + q_r + q_e}$$

### 3.7 STILL EFFICIENCY

A measure of the performance of a still is the conversion efficiency, defined as the ratio of heat transferred in condensation process over any time period to the incident solar energy over the same time period<sup>16</sup>,

i.e.

$$\eta = \frac{\int q_e d\tau}{\int I_s d\tau}$$

where,  $I_s$  = total incident solar radiation (direct + diffuse) falling on the inclined surface under consideration.

$\tau$  = time period.

## CHAPTER - 4

### RESULTS AND DISCUSSIONS

#### 4.1 EXPERIMENTAL PROCEDURE

Experiments on both the inclined and the basin-type stills were carried out over the month of May, 1981, and the data obtained for clear days of uninterrupted sunshine, only, are presented here.

The storage tank was filled every morning with saline water at a concentration of 2.5 gms of salt dissolved per litre of solution. The basins of both the stills were filled next with saline water to a depth of about 1 cm. The saline water inlet valve is then adjusted to maintain a thin film of water flowing over the glass cover, lasting till the end of the day, when the tank becomes nearly empty. The glass cover surface was periodically treated with dilute hydrochloric acid to maintain the uniform flow of water and to prevent the formation of dry patches. Readings were taken at hourly intervals of time, starting from 9.00 a.m. till 5.00 p.m.

The inclined still was tested under two modes of operations :

- (i) The top glass cover was retained. This resulted in low yield of distillate but the temperature of hot water available as a by-product was high (about 44°C).

(ii) The top glass cover was removed. The yield of distillate was high but the hot water temperature was low (about 39 °C). Tables 4.1, 4.2 and 4.3 present the experimental data and the results obtained for the two modes of tests carried out on typical summer days.

#### 4.2 ANALYSIS OF THE EXPERIMENTAL DATA AND RESULTS

A graphical representation of the experimental data for the first mode of test is shown in Fig. 4.1. The hourly total insolation on the inclined still is plotted alongwith the temperatures obtained. From the graph, it is seen that the maximum temperatures of the basin surface ( $T_1$ ), glass cover ( $T_2$ ) and the back surface ( $T_b$ ) are reached sometime after 1 p.m., an hour after the period of maximum insolation. After attaining the maximum temperatures, the curves drop due to the decrease in incoming radiation and increase in heat losses from the basin to the ambient.

The saline water exit temperature,  $T_{w_0}$  shows a continuous rise till about 3 p.m. after which it starts decreasing. This may be explained as follows : The rate of discharge of saline water from the storage tank is non-linear in nature as is evident from column-3 of Table 4.1(b). In the morning hours, when the tank is nearly full, the mass flow rate is high and the upward heat fluxes are low due to low intensity of radiation during this period of the day. Hence,

Table 4.1(a): Experimental data obtained for the Inclined still  
for the first mode of test (top glass cover  
retained)

May 26, 1981

$\Theta = 12^\circ$

	Basin	Bottom	Top	Back	Ambient	Flowing saline	
	water tempe- rature $T_1$ ( $^\circ$ C)	glass cover tempe- rature $T_2$ ( $^\circ$ C)	glass cover tempe- rature $T_g$ ( $^\circ$ C)	surface tempe- rature $T_b$ ( $^\circ$ C)	tempe- rature $T_a$ ( $^\circ$ C)	water tempera- ture Inlet $T_{w_i}$ ( $^\circ$ C)	water tempera- ture Outlet $T_{w_o}$ ( $^\circ$ C)
9 am	42	35	33	34	32	32	33
10 am	48	41	34	37	34	33	35
11 am	53	45	36	40	35	34	37
12 noon	57	49	37	43	36	35	40
1 pm	59	53	39	45	37	36	42
2 pm	58	51	40	45	38	37	43
3 pm	54	47	40	43	37	37	44
4 pm	51	44	39	41	36	37	43
5 pm	49	42	38	39	35	36	42

Table 4.1(b) : Results of the test conducted on May 26, 1981 ( $\theta = 12^\circ$ )

Time	Total Inso- lation on the Incli- ned still, $I_c$ $\frac{W}{m^2 \cdot hr}$	Wind velo- city, $v$ $m$ $\frac{m}{sec}$	Mass Flow rate of sal- ine water, $\dot{m}$ $kg$ $\frac{hr}{m}$	Heat Flux due to Con- vection, $q_c$ $\frac{W}{m^2 \cdot hr}$	Heat Flux due to Radia- tion, $q_r$ $\frac{W}{m^2 \cdot hr}$	Heat Flux due to Evapora- tion, $q_e$ $\frac{W}{m^2 \cdot hr}$	Heat Flux due to Back Losses, $q_b$ $\frac{W}{m^2 \cdot hr}$	Heat Flux from glass cover to ambient	Heat Flux from glass cover to Inclined still	Distillate output from Inclined still	Effecti- veness of heat removal, $E$	Effici- ency of Inclined still				
								$q_e$ exp $\frac{W}{m^2 \cdot hr}$	$q_e$ cal $\frac{W}{m^2 \cdot hr}$	$q_e$ th $\frac{W}{m^2 \cdot hr}$	$N_{exp}$ $\frac{ml}{hr}$	$N_{th}$ $\frac{ml}{hr}$	$\eta_{exp}$ %			
10 am	2102	1.3	29.0	120.6	160.0	870.1	702.7	22.8	474.5	255	130	105	90	0.52	41.4	33.4
11 am	2340	1.55	29.0	116.3	167.8	1073.9	965.5	27.6	406.8	260.6	161	145	140	0.67	45.9	31.3
11 am	3006	1.24	26.5	132.1	218.3	1525.7	1392	32.4	404.6	284.4	230	210	215	0.77	50.3	46.2
12 noon	2988	1.24	23.0	111.2	180.7	1552.3	1519	33.6	334.8	310.3	235	230	230	0.82	52	50.8
1 pm	2862	1.0	19.0	110.9	182.5	1605.2	1484	33.6	453.2	329	243	235	250	0.75	56.1	51.9
2 pm	2628	0.67	17.0	112.6	177.5	1416.6	1390	27.6	382	337.3	214	210	195	0.77	53.9	52.0
3 pm	1336	1.15	15.0	114.5	172.5	1248	1128	26.4	274.7	577.3	186	170	120	0.81	68.0	61.5
4 pm	1526	1.20	11.0	116.3	167.8	1072.8	999	24.0	514.8	377	161	150	90	0.60	70.3	65.4

th - theoretical, exp - experimental, cal - calculated, m - measured.

the exit temperature,  $T_{w_0}$  of the flowing saline-water, is low. With the gradual decrease in the mass flow rate and increase in the upward heat fluxes during the day, more amount of heat is to be removed by less quantity of water. This results in higher exit temperature, during the later part of the day, till about 3 p.m. After 3 p.m., further decrease in the mass flow rate is accompanied by a decrease in the upward heat fluxes due to low intensity of radiation in the evening hours. This causes a gradual decrease in temperature,  $T_{w_0}$ .

The temperature of the saline-water inside the storage tank gradually rises (about  $4^{\circ}\text{C}$  -  $5^{\circ}\text{C}$  throughout the day) due to absorption of heat from the surroundings, but reaches a steady-state after 2 p.m.

The experimental data and the results for the second mode of test are given in Tables 4.2(a) and 4.2(b), respectively, and are plotted in Fig. 4.2. From the graph it is observed that the general pattern of the temperature profiles is similar to that in Fig. 4.1. However, the flowing saline-water outlet temperature,  $T_{w_0}$  shows a marked decrease of about  $2^{\circ}\text{C}$  -  $8^{\circ}\text{C}$  throughout the day. This is due to the rapid cooling of the water-film as its surface is being constantly exposed to the ambient. The temperature,  $T_2$  of the condensation surface, is further reduced due to the cooling by the water-film, resulting in higher yield of distillate and better efficiency of conversion.

Table 4.2(a): Experimental data obtained for the Inclined still for the second mode of test (top glass cover removed)  
May 27, 1981

$$\theta = 12^\circ$$

	Basin water tempe- rature $T_1$ ( $^{\circ}$ C)	Glass cover tempe- rature $T_2$ ( $^{\circ}$ C)	Back surface tempe- rature $T_b$ ( $^{\circ}$ C)	Ambient tempe- rature $T_a$ ( $^{\circ}$ C)	Flowing saline water temperature	
					Inlet $T_{w_i}$ ( $^{\circ}$ C)	Outlet $T_{w_o}$ ( $^{\circ}$ C)
9 am	43	34	34	31	32	32
10 am	49	40	36	32	33	34
11 am	54	45	39	35	34	36
12 noon	58	49	42	36	35	38
1 pm	60	51	43	37	36	39
2 pm	58	50	43	37	36	39
3 pm	54	46	41	37	36	39
4 pm	50	42	39	36	36	37
5 pm	46	39	37	35	36	34

Table 4.2(b) : Results of the test conducted on Oct. 07, 1931 (6 p.m.)

Total Impala- tion Rate on the In- clined Surface, $I_s$	Wind Velocity in ft. sec. m. sec	Mass Flow Rate of Gallons Water per min	Heat Flux due to Convec- tion, W/m <sup>2</sup>	Heat Flux due to Radiation, W/m <sup>2</sup>	Heat Flux due to Back Jackets, W/m <sup>2</sup>	Heat Flux from Inclined Surface		Heat Flux from Back Jackets		Heat Flux from Radiant Jackets		Heat Flux from Back Jackets		Heat Flux from Radiant Jackets		Heat Flux from Back Jackets		Heat Flux from Radiant Jackets	
						$q_{th}$	$q_{exp}$	$q_{th}$	$q_{exp}$	$q_{th}$	$q_{exp}$	$q_{th}$	$q_{exp}$	$q_{th}$	$q_{exp}$	$q_{th}$	$q_{exp}$	$q_{th}$	$q_{exp}$
9 am- 10 am	1800	1.9	26.5	143.1	205.8	1253	1038	26.4	187	155	70	69.6	57.7						
10 am- 11 am	2250	1.75	28.0	162.7	217.8	1614.6	1431.7	33.6	242.5	215	125	71.8	63.6						
11 am- 12 noon	2945	1.6	27.0	158.3	226	1902.6	1757.5	37.2	266.8	265	215	64.4	59.7						
12 noon- 1 pm	37	22.5	156.2	252.2	2191.7	1950.8	39.6	332.4	295	260	72.5	64.5							
1 pm- 2 pm	2592	1.5	13.0	135.2	207.8	1895.8	1816.6	38.4	237	275	240	71.1	71.1						
2 pm- 3 pm	2576	1.3	16.0	135.1	202	1635	1490.6	33.5	249.8	225	165	60.7	52.7						
3 pm- 4 pm	1915	0.9	14.0	172.4	194.4	1411.2	1264	23.8	212.1	190	115	73.7	56.0						
4 pm- 5 pm	1429	1.2	10.0	118.2	164.7	1015.2	800	24.0	152	120	65	71.0	56.0						

th. = theoretical, exp. = experimental.

Figures 4.3 and 4.4 show the hourly variation of still output obtained for the first and second modes of tests, respectively. From the graphs, it is found that the difference between the theoretical and experimental output of distillate for the inclined still varies from 3 per cent - 20 per cent in case of the first mode of test and 7 per cent - 21 per cent for the second mode of test conducted over the entire period of the day, from 9 a.m. to 5 p.m. The difference in the theoretical and experimental results may be due to the following reasons:

- (i) loss of distillate due to leakage of water-vapour through the linings and dropping of condensate from the glass cover to the basin,
- (ii) loss of distillate during pouring and transferring while taking measurements, and
- (iii) the thin film of condensate adhering to the bottom surface of the glass cover has not been taken into account.

Figure 4.5 shows a comparative study of the cumulative yield for a day for the basin type and the inclined still for the first mode of test. It is seen that the yields of the stills are nearly the same till about 12 noon, after which the yield from the inclined still keeps on gradually increasing for the rest of the day. The total increase in the yield of the inclined still over the basin-type unit is about 10 per cent. From Fig. 4.6, it is found that for the second mode of test

CENTRAL LIBRARY  
No. A 70577

when the top glass cover is removed, the total increase in the yield of the inclined still over the basin-type is about 38 per cent. A comparison between Figures 4.5 and 4.6 shows that the cumulative yield of the inclined still in case of the second mode of test is about 17 per cent higher as compared to that of the first mode. This increase in yield in the second mode of test is due to the facts that the bottom glass cover is cooled more effectively by the water film exposed to the ambient and also due to improved evaporation rate of saline water as a result of increased intensity of radiation falling on the basin.

The theoretical as well as the experimental values of efficiency of conversion of saline water into fresh water for the inclined still are plotted over the day for the first mode of test and shown in Fig. 4.7. It is observed that the efficiency of conversion increases during the later part of the day. This may be explained as follows :

Since, the rate of upward heat flux (analogous to the upward heat losses from a collector plate to the ambient) due to the combined effects of convection, radiation and evaporation increases with the decrease in the intensity of solar radiation during the later part of the day, the still efficiency ( $q_e/I_s$ ) also increases. The theoretical and experimental efficiencies for the second mode of test are plotted in Fig. 4.8. The trend, in this case, is somewhat uniform throughout the day. Comparing the experimental results of Figures 4.7 and 4.8, it is found

Table 4.3 : Comparison of daily total yield of distillate for the two types of stills for the month of May, 1981

	Daily Total Insolation (KWh/m <sup>2</sup> -day)	Daily Total yield of Inclined still for 1st mode of test (top glass cover retained) (litres/m <sup>2</sup> -day)	Daily Total yield of Inclined still for 2nd mode of test (top glass cover removed) (litres/m <sup>2</sup> -day)	Daily Total yield of Basin-type still (litres/m <sup>2</sup> -day)
May 11	4.7	3.95	-	3.45
12	4.6	-	4.25	-
13	-	-	-	3.40
14	4.8	3.85	-	-
15	4.75	-	4.2	3.7
16	4.4	3.80	-	-
17	4.7	-	4.3	3.7
18	4.6	4.05	-	3.45
19	4.75	-	4.3	3.45
20	-	-	-	-
21	4.90	4.0	-	-
22	4.80	-	4.7	3.4
23	5.10	4.2	-	-
24	5.25	-	4.9	3.6
25	-	-	-	-
26	5.25	4.0	-	3.65
27	5.10	-	4.80	3.5
28	5.30	4.0	-	3.6
29	4.90	-	4.60	3.55
30	5.10	3.95	-	-
31	5.0	-	4.75	3.7

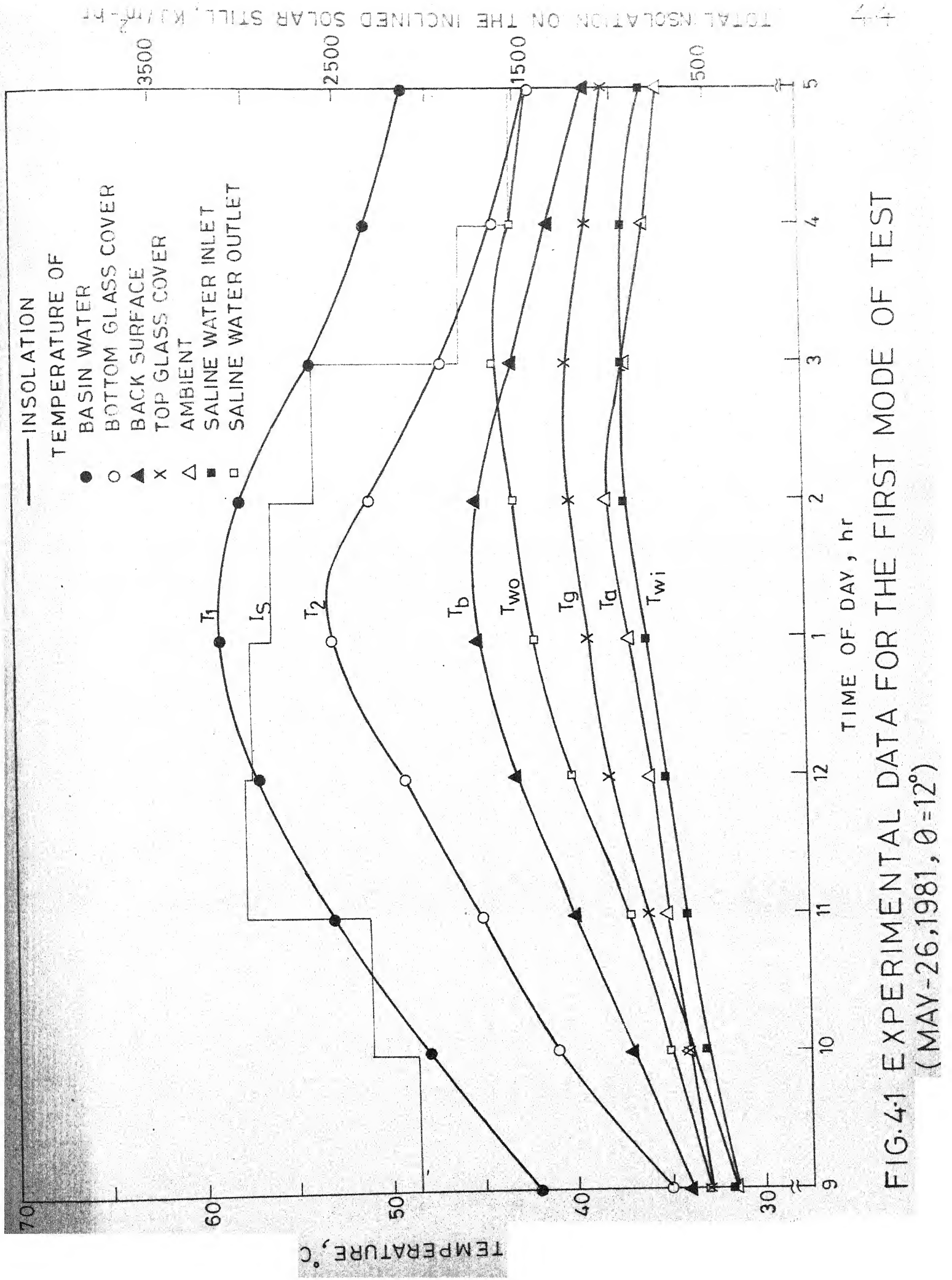


FIG. 4.1 EXPERIMENTAL DATA FOR THE FIRST MODE OF TEST  
(MAY-26,1981,  $\theta=12^{\circ}$ )

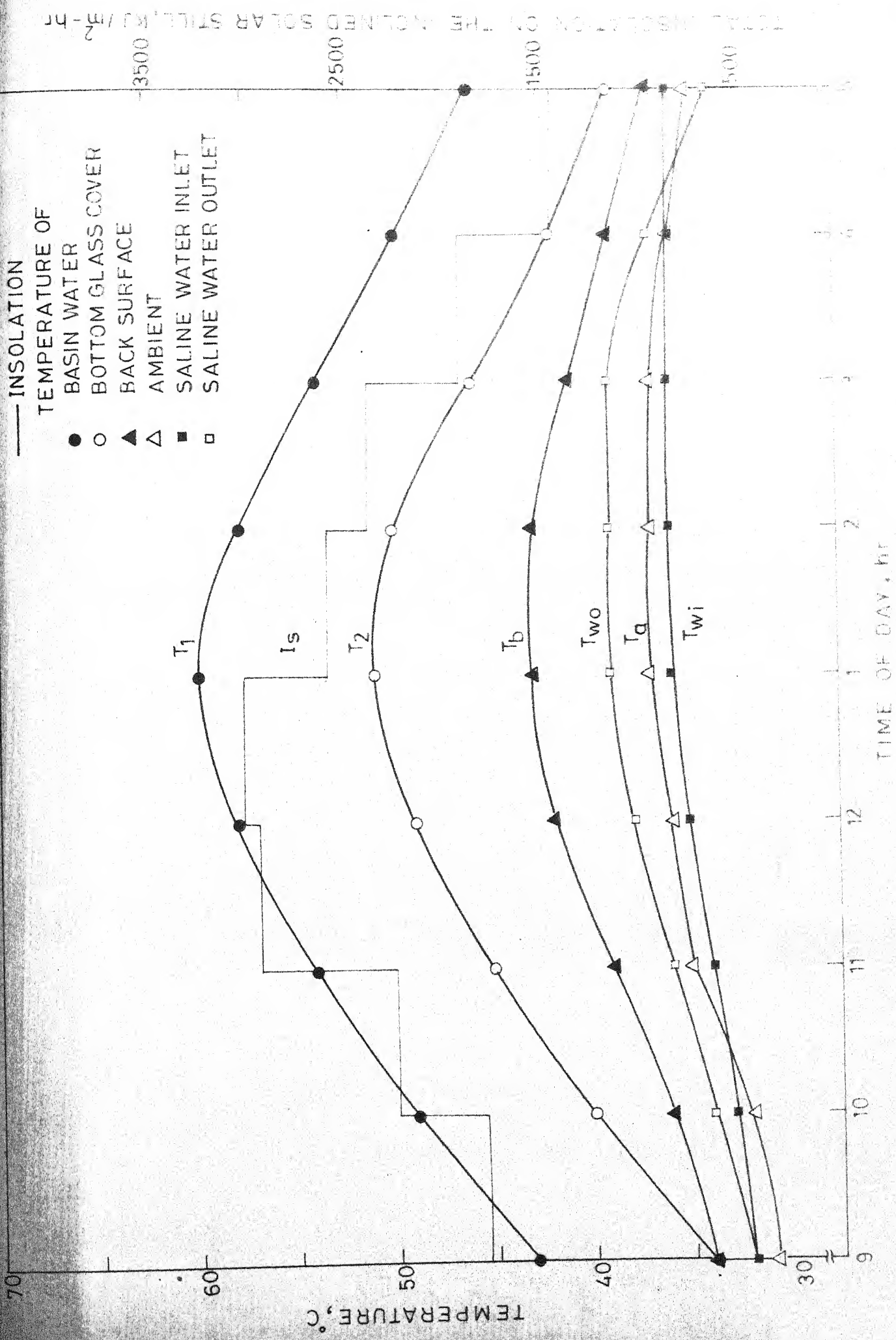


FIG. 4.2 EXPERIMENTAL DATA FOR THE SECOND MODE OF TEST  
(MAY-27, 1981  $\theta = 12^\circ$ )

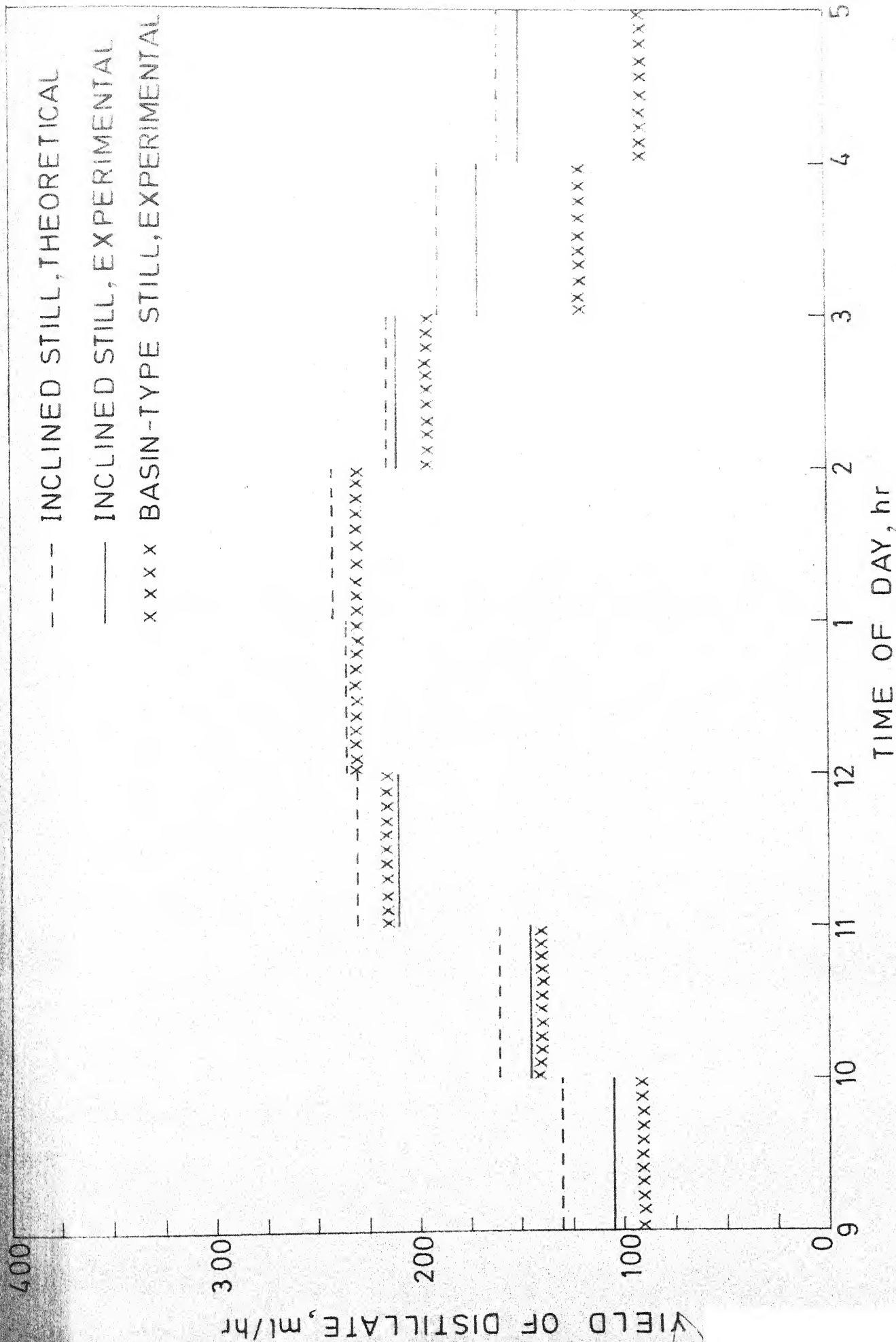


FIG. 4.3 VARIATION OF HOURLY YIELD OF DISTILLATE OVER THE DAY FOR THE FIRST MODE OF TEST (MAY 26, 1981)

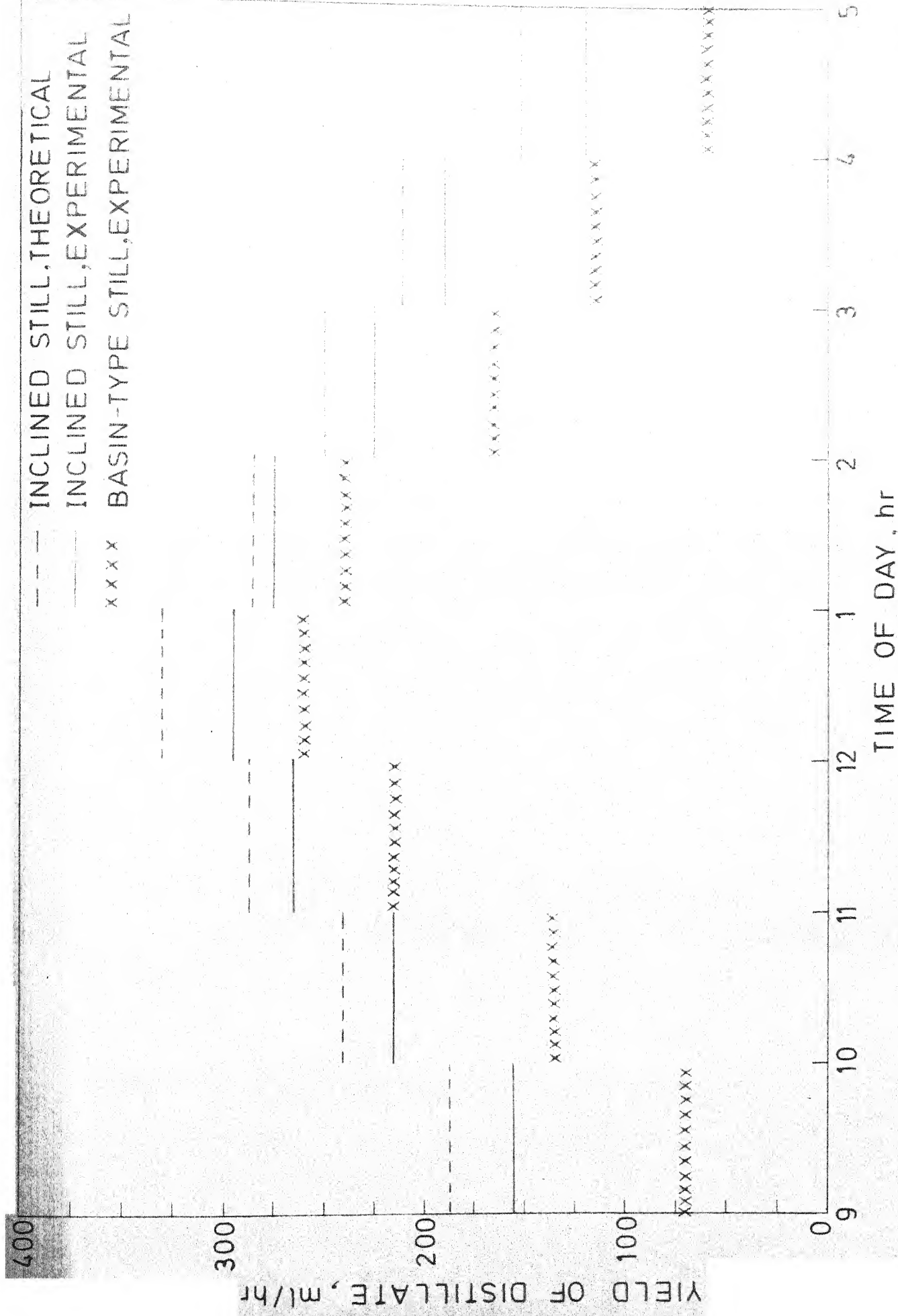


FIG. 4.4 VARIATION OF HOURLY YIELD OF DISTILLATE OVER TIME (MAY 27, 1981)  
FOR THE SECOND MODE OF TEST (MAY 27, 1981)

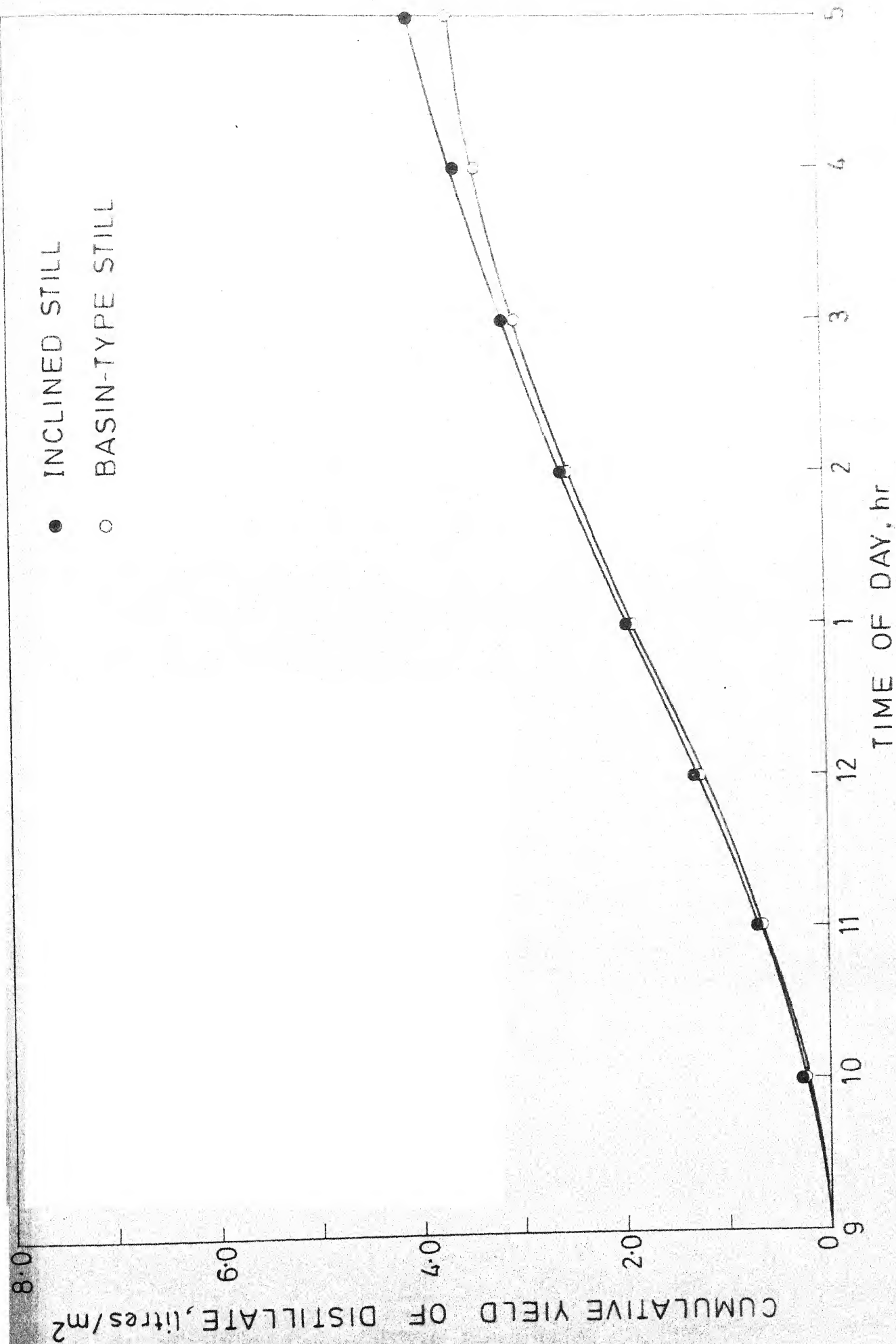


FIG. 4.5 VARIATION OF CUMULATIVE YIELD OF DISTILLATE OVER THE DAY FOR THE FIRST MODE OF TEST (MAY 26, 1981)

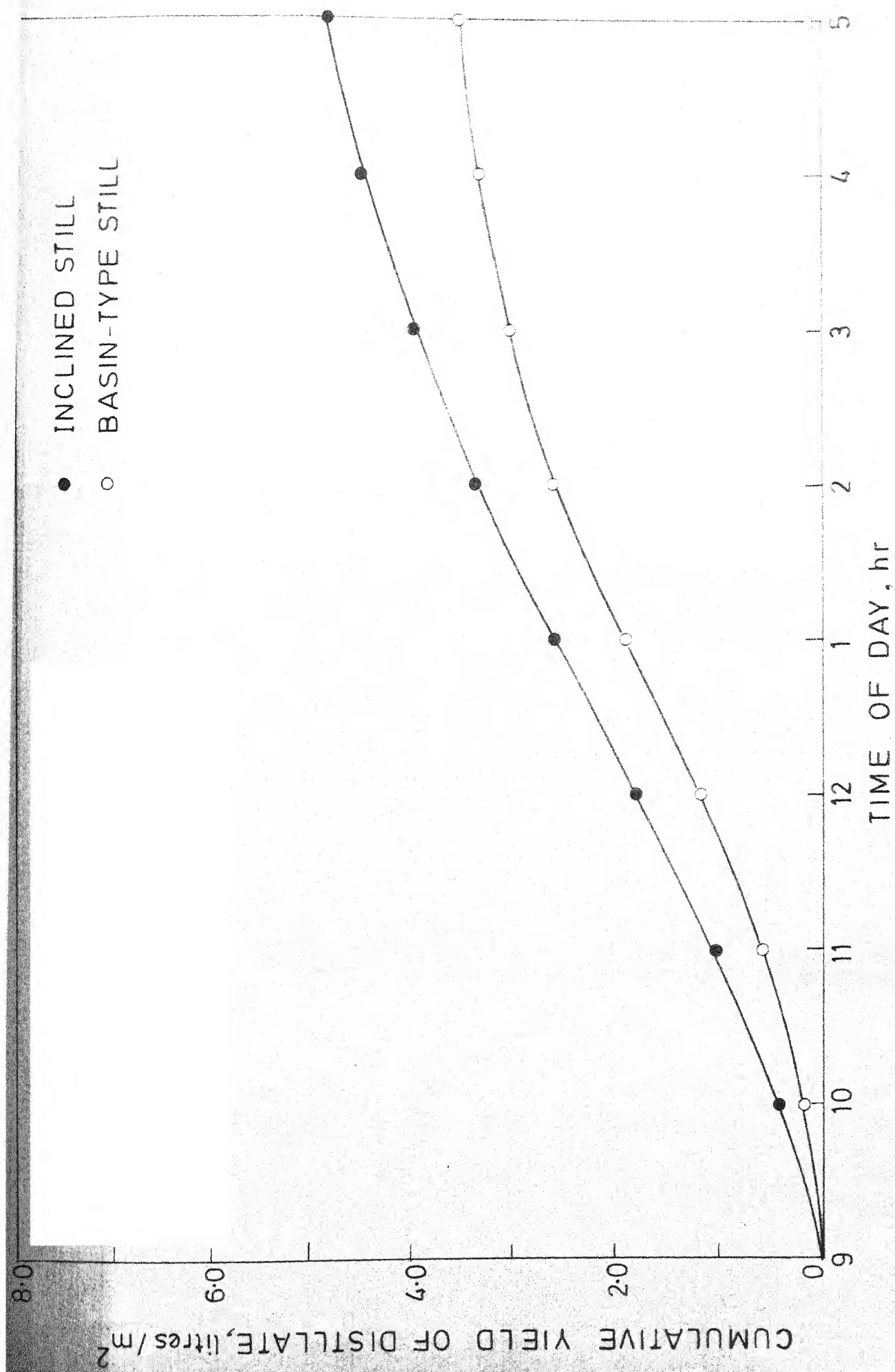


FIG. 4.6 VARIATION OF CUMULATIVE YIELD OF DISTILLATE OVER THE DAY FOR THE SECOND MODE OF TEST (MAY 27, 1981)

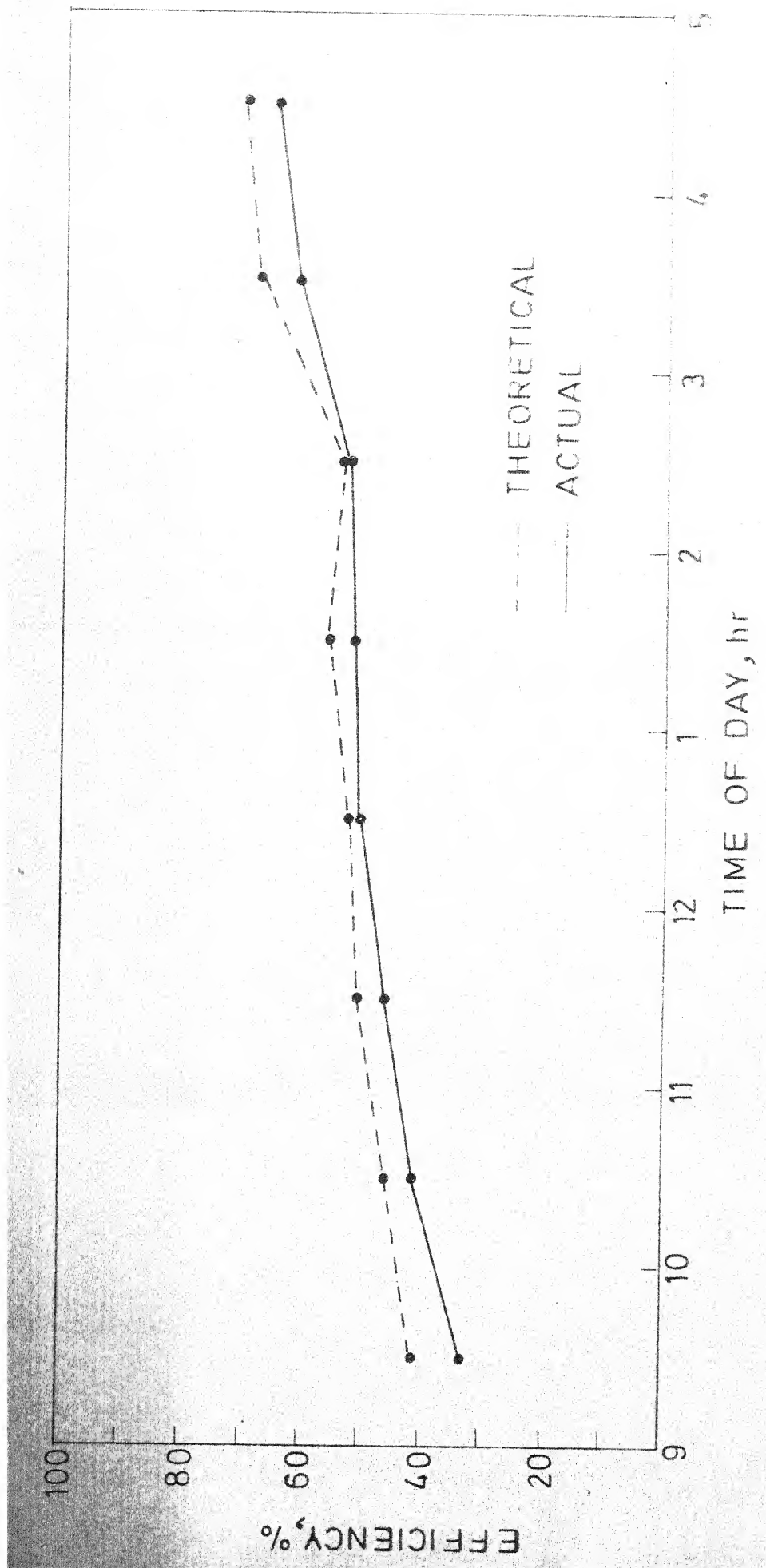


FIG. 4.7 COMPARISON OF THE THEORETICAL AND ACTUAL EFFICIENCIES OF CONVERSION FOR THE FIRST MODE OF TEST FOR THE INCLINED STILL (MAY 26, 1981)

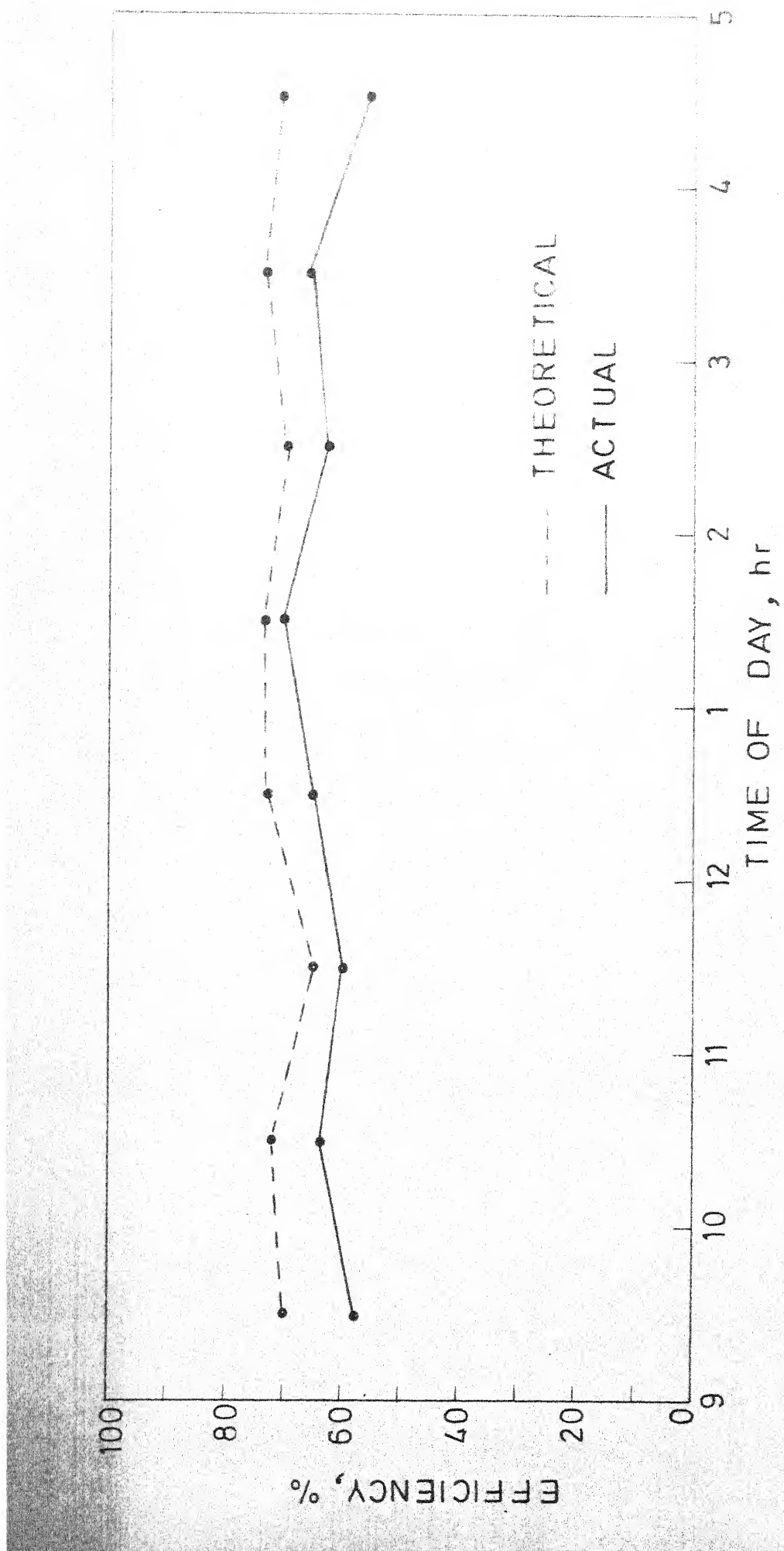


FIG. 4.8 COMPARISON OF THE THEORETICAL AND ACTUAL EFFICIENCIES OF CONVERSION FOR THE SECOND MODE OF TEST FOR THE INCLINED STILL (MAY 27, 1981)

○ FIRST MODE OF TEST  
● SECOND MODE OF TEST

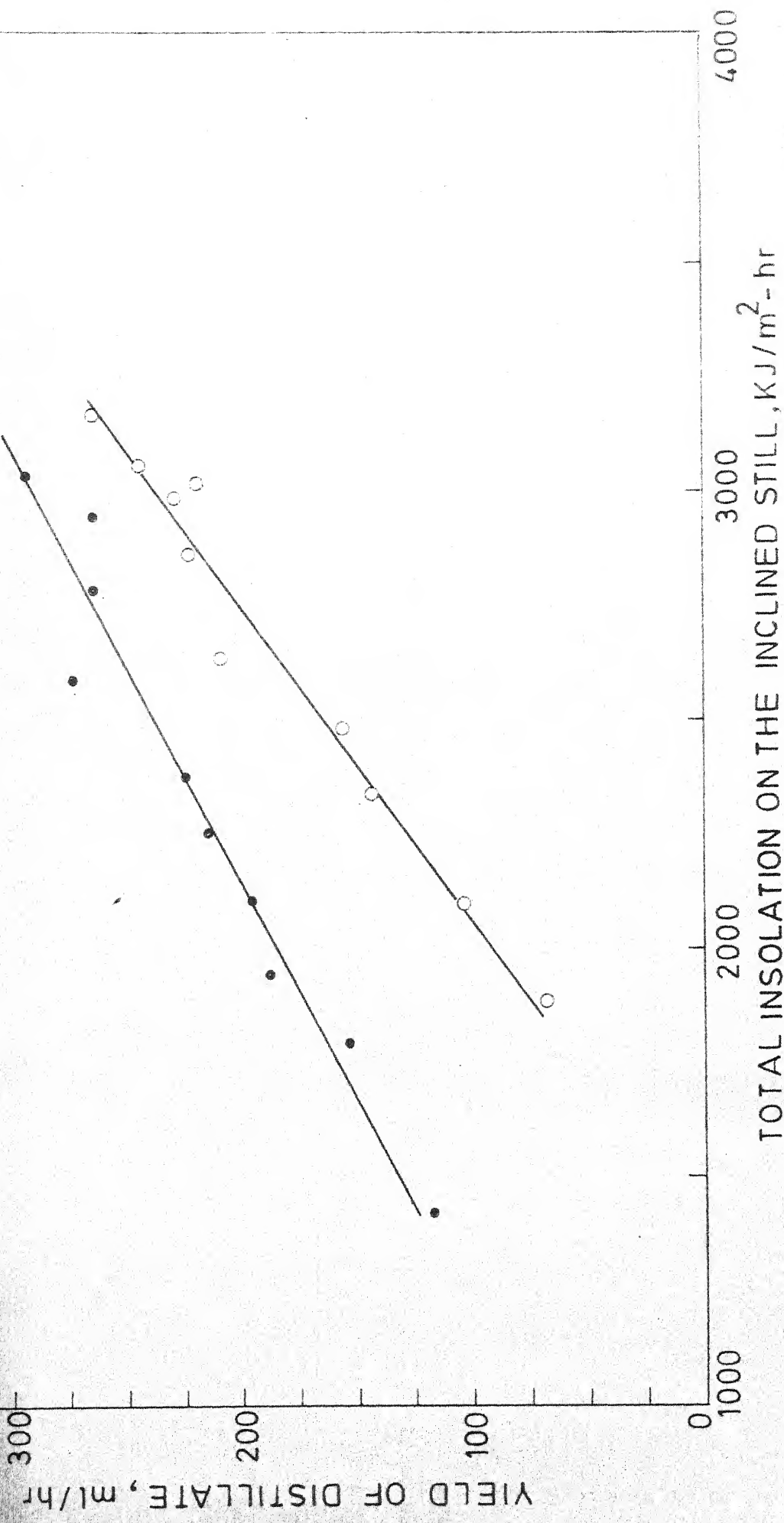


FIG. 4.9 VARIATION OF YIELD OF DISTILLATE OVER TOTAL INSOLATION FOR THE INCLINED STILL

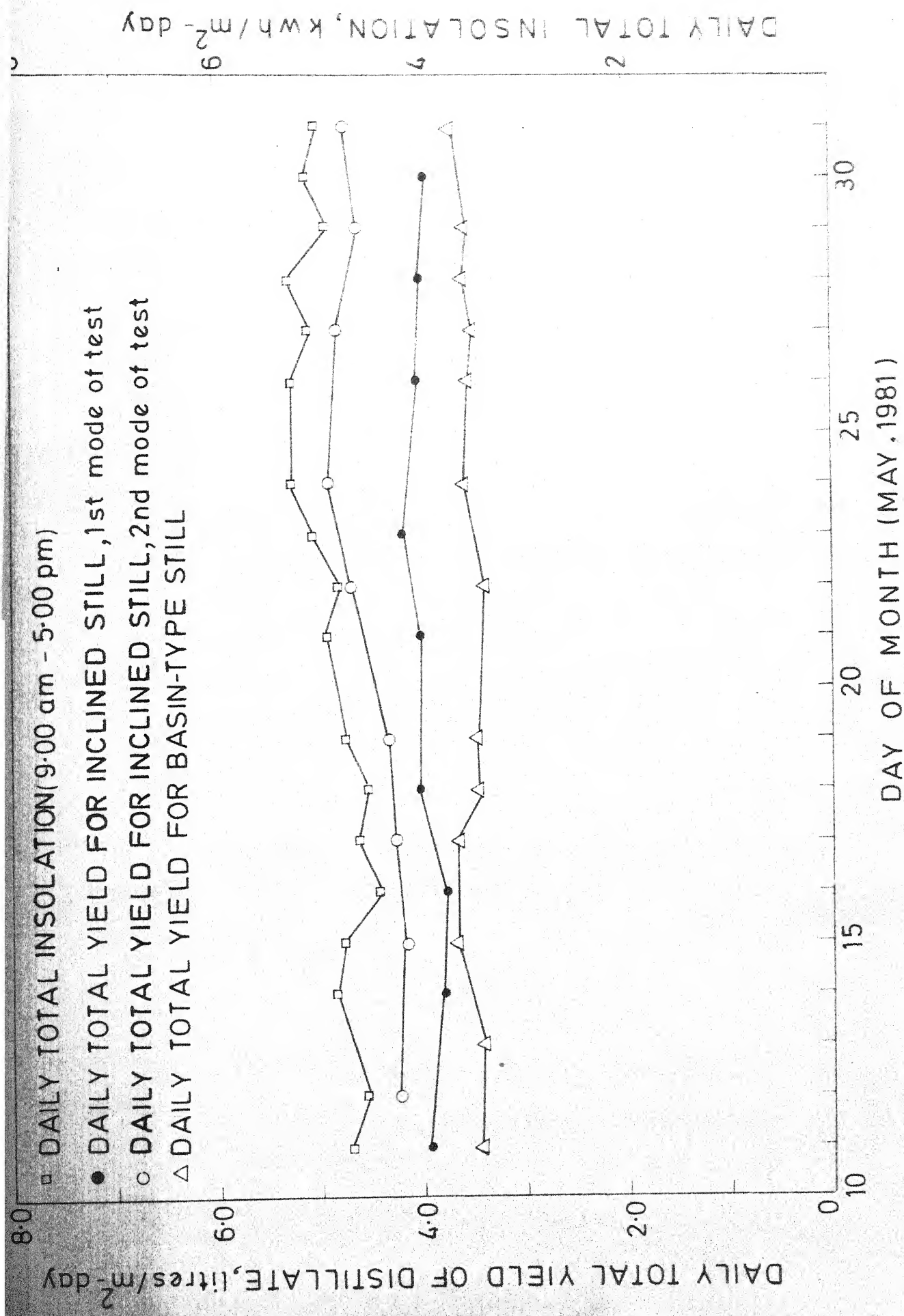


FIG.4.10 COMPARISON OF DAILY TOTAL YIELD OF DISTILLATE FOR THE MONTH OF MAY ,1981

that the efficiency in the second mode of test varies between 55 per cent - 70 per cent against 35 per cent - 65 per cent in case of the first mode.

A comparison of the yield of distillate for the two modes of tests against various values of total insolation on an inclined still is shown in Fig. 4.9. Such a graph is useful in the prediction of distillate yield on an hourly, daily or monthly basis, for various values of the intensity of radiation. However, extensive data are required for accurate prediction of such results.

Finally, the experimental results obtained for the daily total insolation and yield of distillate for the two types of stills during the month of May, 1981 are given in Table 4.3 and plotted in Fig. 4.10.

#### 4.3 CONCLUSIONS

The following conclusions may be drawn on the basis of the study carried out on both the inclined and basin-type solar stills :

- (1) The inclined solar still combines the process of desalination and hot-water production. The heat which is normally dissipated to the ambient in a conventional solar still is utilized here effectively to obtain hot-water on a continuous basis at temperatures varying between 40 °C to 50 °C, throughout the day.

- (2) The process of cooling the bottom glass cover by the flowing saline water results in high yield of distillate and consequently, high conversion efficiency. Efficiencies more than 70 per cent have been attained for the second mode of test during the month of May.
- (3) The experimental results obtained for the inclined solar still match well in most cases with those obtained from theoretical analysis. The theoretical model may be further improved by taking into account the transient effects occurring inside the still.
- (4) The inclined solar still may be used for either mode of operation, depending upon the need of the user. The first mode of operation, which necessitates the use of an extra glass cover is justified in view of the hot-water production, since it results in only a marginal increase in the capital cost of the still.
- (5) The major accessory of the inclined solar still is the saline-water storage tank, which slightly increases the capital cost. However, in actual practice, large basins may be constructed along sea-coasts which will be filled up during high tides by sea water. The saline water will then be fed through pipes continuously into the inclined stills installed over a vast area. Such a scheme, if implemented, may result in the production of large quantities of fresh water economically in future.

## REFERENCES

1. MARIA TELKES, Solar Stills, Proceedings of the World Symposium on Applied Solar Energy, Phoenix, Arizona, 1955, pp. 73-79.
2. W. SZULMAYER, Solar Stills With Low Thermal Inertia, Solar Energy, Vol. 14, No. 4, March 1973, pp. 415-421.
3. V.R. MUTHUVEERAPPAN and G. KAMARAJ, Mini Solar Still for Rural Applications, Proceedings of the International Solar Energy Society Congress, New Delhi, India, 1978, pp. 2036-2040.
4. PIO C. LOBO and Rde SEVERINO ARAÚJO, A Simple Multi-effect Basin-type Solar Still, Proceedings of the International Solar Energy Society Congress, New Delhi, India, 1978, pp. 2026-2030.
5. R.A. AKHTAMOV et al., Study of Regenerative Inclined-Stepped Solar Still, Applied Solar Energy (Gelioteckhnika), Vol. 14, No. 4, 1978, pp. 41-44.
6. R.V. DUNKLE, Solar Water Distillation : The Roof-type Still and a Multiple-effect Diffusion Still, Int. Dev. Heat Transfer, ASME, 1961, pp. 895-902.
7. K.G.T. HOLLANDS et al., Free Convection across Inclined Air Layers with one Surface V-corrugated, Journal of Heat Transfer, August 1978, pp. 410-415.
8. W.R. WILCOX, Simultaneous Heat and Mass Transfer in Free Convection, Chemical Engineering Science, Vol. 13, 1961, pp. 113-119.

9. R.E. TREYBAL, Mass-Transfer Operations, 2nd Edition, McGraw-Hill, 1968, pp. 55-59.
10. J.R. WELTY, C.E. WICKS and R.E. WILSON, Fundamentals of Momentum, Heat and Mass Transfer, Wiley International Edition, 1969, p. 556.
11. R.B. BIRD, W.E. STEWARD and E.N. LIGHTFOOT, Transport Phenomena, John-Wiley and Sons, Inc., 1960, pp. 636-640.
12. MAX JACOB and GEORGE A. HAWKINS, Elements of Heat Transfer, 3rd Edition, John-Wiley and Sons, Inc., 1957, p. 283.
13. E.R.G. ECKERT and R.M. DRAKE, Jr., Heat and Mass Transfer, 2nd Edition, Tata McGraw-Hill, 1979, pp. 500-504.
14. ROBERT H. PERRY and CECIL H. CHILTON, (Ed), Chemical Engineers' Handbook, 5th Edition, McGraw-Hill, 1973, pp. 3-230-3-233, p. 3-206.
15. A.A.M. SAYIGH (Ed), Solar Energy Engineering, Academic Press, 1977, p. 452.
16. FRANK KREITH and JAN F. KREIDER, Principles of Solar Engineering, McGraw-Hill, 1978, p. 547.

APPENDIX - 1EVALUATION OF THE BUOYANCY FACTORS FOR HEAT AND MASS  
TRANSFERS IN NATURAL CONVECTION

Let  $\mathbf{v}$  be the volume of the enclosure occupied by the mixture in the inclined still.

and,

$\mathbf{m}$  the total mass of the mixture

$m_A, m_B$  - masses of water-vapour and air in the mixture, respectively

$M_A, M_B$  - molecular weights of water-vapour and air, respectively

$p$  - total pressure of the mixture

$p_A, p_B$  - partial pressures of water-vapour and air, respectively

$T$  - mean temperature of the mixture

$\rho, \rho_A, \rho_B$  - densities of mixture, water-vapour and air, respectively

$\mathbf{v}, v_A, v_B$  - specific volumes of mixture, water-vapour, and air, respectively

The coefficient of volume expansion for the mixture is given by

$$\beta_t = \frac{1}{\mathbf{v}} \left( \frac{\partial \mathbf{v}}{\partial T} \right)_p$$

Linearizing the above expression,

$$\beta_t \approx \frac{1}{v_2} \left( \frac{v_1 - v_2}{T_1 - T_2} \right),$$

where, the subscripts 1 and 2 refer to the lower and upper

surfaces of the enclosure, respectively.

or,

$$\begin{aligned}
 \beta_t (T_1 - T_2) &= \frac{v_1 - v_2}{v_2} \\
 &= \frac{\frac{1}{\rho_1} - \frac{1}{\rho_2}}{\frac{1}{\rho_2}} \\
 &= \frac{\rho_2}{\rho_1} - 1 \quad (i)
 \end{aligned}$$

Applying the ideal gas law to water-vapour and air, we obtain,

$$p_A V = \frac{m_A}{M_A} R_u T \quad (ii)$$

$$p_B V = \frac{m_B}{M_B} R_u T \quad (iii)$$

where  $R_u$  = Universal Gas Constant.

From (ii),  $\frac{m_A}{V} = \frac{p_A M_A}{R_u T}$

From (iii),  $\frac{m_B}{V} = \frac{p_B M_B}{R_u T}$

Adding,  $\frac{m_A + m_B}{V} = \frac{1}{R_u T} [ p_A M_A + p_B M_B ]$

i.e.  $\frac{m}{V} = \frac{1}{R_u T} [ p_A M_A + p_B M_B ]$

or,  $\rho = \frac{1}{R_u T} [ p_A M_A + p_B M_B ]$

Hence, Eqn. (i) can be written as

$$\beta_t(T_1 - T_2) = \frac{T_1}{T_2} \left[ \frac{p_{A_2} \frac{M_A}{M_A} + p_{B_2} \frac{M_B}{M_B}}{p_{A_1} \frac{M_A}{M_A} + p_{B_1} \frac{M_B}{M_B}} \right] - 1 \quad (\text{iv})$$

From Dalton's Law of partial pressures,

$$p_A + p_B = p$$

Eqn. (iv) can be expressed as

$$\begin{aligned} \beta_t(T_1 - T_2) &= \frac{T_1}{T_2} \left[ \frac{p_{A_2} \frac{M_A}{M_A} + (p - p_{A_2}) \frac{M_B}{M_B}}{p_{A_1} \frac{M_A}{M_A} + (p - p_{A_1}) \frac{M_B}{M_B}} \right] - 1 \\ &= \frac{T_1}{T_2} \left[ \frac{p_{A_2} \frac{M_A}{M_A} + (p - p_{A_2}) \frac{M_B}{M_B} + p_{A_1} \frac{M_A}{M_A} - p_{A_1} \frac{M_A}{M_A} - p_{A_1} \frac{M_B}{M_B} + p_{A_1} \frac{M_B}{M_B}}{p_{A_1} \frac{M_A}{M_A} + (p - p_{A_1}) \frac{M_B}{M_B}} \right] - 1 \end{aligned}$$

After rearranging terms and simplifying,

$$\begin{aligned} \beta_t(T_1 - T_2) &= \frac{T_1}{T_2} \left[ 1 + \frac{(p_{A_1} - p_{A_2}) (M_B - M_A)}{(M_B p - p_{A_1}) (M_B - M_A)} \right] - 1 \\ &= \frac{T_1}{T_2} \left[ 1 + \frac{\frac{p_{A_1} - p_{A_2}}{M_B p}}{\frac{M_B - M_A}{M_B - M_A} - p_{A_1}} \right] - 1 \\ &= \frac{T_1 - T_2}{T_2} + \left[ \frac{\frac{p_{A_1} - p_{A_2}}{M_B p}}{\frac{M_B - M_A}{M_B - M_A} - p_{A_1}} \right] \frac{T_1}{T_2} \quad (\text{v}) \end{aligned}$$

The coefficient of densification,  $\beta_m$  is defined as follows:

$$\beta_m = -\frac{1}{\rho} \left( \frac{\partial \rho}{\partial c} \right)_T \quad (vi)$$

where  $c$  denotes the mixture concentration. The negative sign indicates that with the increase in the concentration of water-vapour in air, the mixture density, decreases, owing to the fact that moist air is lighter than dry air.

Linearizing the above expression,

$$\beta_m = -\frac{1}{\rho_2} \left( \frac{\rho_1 - \rho_2}{c_1 - c_2} \right)$$

$$\text{or, } \beta_m (c_1 - c_2) = 1 - \frac{\rho_1}{\rho_2} \quad (vii)$$

Applying ideal gas law to both water-vapour and air and proceeding in a similar may was before, we obtain, finally

$$\beta_m (c_1 - c_2) = \frac{T_1 - T_2}{T_1} + \left[ \frac{\frac{p_{A1} - p_{A2}}{M_B p}}{\frac{M_B - M_A}{M_B} - \frac{p_{A2}}{M_A}} \right] \frac{T_2}{T_1} \quad (viii)$$

It has been found that for small differences in temperatures of the two surfaces, buoyancy factors for the heat and mass transfers denoted by the left-hand sides of expressions (v) and (viii) give nearly the same value.

APPENDIX - 2

## COMPUTER PROGRAMME

\*\*\*\*\*  
 THIS PROGRAMME COMPUTES THE MASS TRANSFER RATE AND  
 THE HEAT FLUXES DUE TO CONVECTION , RADIATION AND  
 EVAPORATION FOR THE INCLINED , SOLAR STILL  
 \*\*\*\*\*

COMMON/AV/RHO(90),XMU(90),XK(90),P(90),HFG(90),T(90)  
 COMMON/BV/AVRHO,AVMU,AVK  
 REAL N1, L, MA, MB  
 DO 10 I = 27,77,1  
 READ \*, T(I),RHO(I),XMU(I),XK(I),P(I),HFG(I)

T REPRESENTS THE TEMPERATURE IN DEGREES CENTIGRADE, RHO, THE DENSITY IN KILOGRAMS PER CUBIC METRES , MU, THE VISCOSITY IN KILOGRAM PER METER PER SECOND , K, THE THERMAL CONDUCTIVITY IN WATTS PER METER PER DEGREE CENTIGRADE , P , THE PRESSURE IN KILOGRAM FORCE PER SQUARE CENTIMETER , AND HFG , THE LATENT HEAT OF CONDENSATION IN KILOCALORIES PER KILOGRAM.

10 XMU(I) = XMU(I)\*1.0E-05  
 CONTINUE  
 DO 30 N = 27,76  
 DO 30 M = N+1,77  
 MM = N ; NN = N  
 CALL AVEG(MM,NN)  
 PRINT 20 ,T(M),T(N),AVRHO,AVMU,AVK,P(M),P(N),HFG(N)

AVRHO,AVMU,AVK REPRESENT THE DENSITY , VISCOSITY AND THERMAL CONDUCTIVITY OF THE AIR IN THE STILL , EVALUATED AT THE AVERAGE TEMPERATURE OF THE EVAPORATING AND CONDENSING SURFACES , RESPECTIVELY.

CP = 1004.10

CP REPRESENTS THE SPECIFIC HEAT OF THE AIR EXPRESSED IN JOULES PER KILOGRAM PER DEGREE CENTIGRADE.

PRINT 25  
 DO 40 IB1 = 1,41  
 IB = IB1-1

IB REPRESENTS THE ANGLE OF TILT OF THE SOLAR STILL WITH THE HORIZONTAL , EXPRESSED IN DEGREES.

MA = 18.02  
 MB = 28.97  
 PT = 1.0332

MA, MB REPRESENT THE MOLECULAR WEIGHTS OF WATER AND AIR ,  
RESPECTIVELY , PT, THE TOTAL PRESSURE INSIDE THE STILL  
EXPRESSED IN KILOGRAM FORCE PER SQUARE CENTIMETER.

$$\text{BUOYT} = (T(M)-T(N))/T(N) + ((P(M)-P(N))/((PT*MB/(MB-MA))-P(N)))*1/(T(M)/T(N))$$

$$\text{BUOYM} = (T(M)-T(N))/T(M) + ((P(M)-P(N))/((PT*MB/(MB-MA))-P(N)))*1/(T(N)/T(M))$$

BUOYT & BUOYM REPRESENT THE BUOYANCY FACTORS FOR HEAT & MASS TRANSFERS , RESPECTIVELY.

$$L = 0.05$$

L REPRESENTS THE DISTANCE IN METRES , BETWEEN THE EVAPORATING AND CONDENSING SURFACES , G , THE ACCELERATION DUE TO GRAVITY IN METRES PER SQUARE SECOND

$$G = 9.81$$

$$GR = G*L*L*AVRHO*AVRHO*BUOYT/(AVMU*AVMU)$$

$$GRM = G*L*L*AVRHO*AVRHO*BUOYM/(AVMU*AVMU)$$

GR, GRM REPRESENTS THE GRASHOF NUMBERS FOR HEAT AND MASS TRANSFERS , RESPECTIVELY

$$RAT = 11300 * (1.0 + 0.204*SIND(4.5*(IB-37.8)))$$

$$PR = AVMU*CP/AVK$$

PR REPRESENTS THE PRANDTL NUMBER

$$D = 1.17E-09*((T(M)+T(N))/2.0+273)**1.75$$

D REPRESENTS THE DIFFUSION COEFFICIENT , EXPRESSED IN SQUARE METER PER SECOND

$$SC = (AVMU/AVRHO)/D$$

SC REPRESENT THE SCMIDT NUMBER

$$HC = AVK/L*(2.44+(2.23-0.123*IB+0.00034*IB*IB)*((GR*PR/RAT*1/COSD(FLOAT(IB)))*(1.0/3.0))-1.0)$$

HC REPRESENTS THE HEAT TRANSFER COEFFICIENT EXPRESSED IN WATTS PER SQUARE METER PER DEGREE CENTIGRADE

$$CON = HC*(T(M)-T(N))$$

12700 C CON REPRESENTS THE HEAT FLUX DUE TO CONVECTION , EXPRESSED IN  
 12800 WATTS PER SQUARE METER.  
 12900  
 13000  
 13100 RAD = 5.103 \* (((T(M)+273)/100)\*\*4 - ((T(N)+273)/100) \*\* 4)  
 13200  
 13300  
 13400  
 13500 RAD REPRESENTS THE HEAT FLUX DUE TO RADIATION , EXPRESSED IN  
 13600 WATTS PER SQUARE METER.  
 13700  
 13800 HD = AVK/L\*(2.44+(2.23-0.123\*IB+0.00034\*IB\*IB)\*((GRM\*SC/RAT\*  
 13900 1 CUSD(FLOAT(IB))\*\*1.0/3.0)-1.0)  
 14000  
 14100 HD REPRESENTS THE MASS -TRANSFER COEFFICIENT , EXPRESSED IN  
 14200 KILOGRAM PER SQUARE METER PER SECOND.  
 14300  
 14400  
 14500  
 14600  
 14700 N1= (5.689E08\*HD/AVRHO)\*(1.0/((T(M)+T(N))/2.0+273))\*(P(M)-P(N))  
 14800  
 14900  
 15000  
 15100 N1 REPRESENTS THE MASS TRANSFER RATE,EXPRESSED IN MILLILITRES  
 15200 PER HOUR  
 15300  
 15400  
 15500  
 15600  
 15700 EVAP = 0.0032283 \* N1 \* HFG(N)  
 15800  
 15900  
 16000  
 16100 PRINT50,IB,BUOYT,BUOYM,RAT,D,GR,GRM,PR,SC,HC,HD,N1,CON,RAD,EVAP  
 16200 40 CONTINUE  
 16300 30 CONTINUE  
 16400 20 FORMAT(//132(1H=)//3X,'IW = ',F4,1,'4X,'TG = ',F4,1,'4X,'RHO = '  
 16500 1,F6.4,'4X,'MU = ',E14.7,'4X,'K = ',F7.5,'4X,'PW = ',F7.5,'4X,'PG  
 16600 2,F7.5,'4X,'HFG = ',F5.1//)  
 16700 50 FORMAT(3X,I2,3X,F4.2,3X,F4.2,3X,F7.1,3X,E8.3,3X,E8.3,3X,E8.3,  
 16800 1F4.2,3X,F4.2,3X,F4.1,3X,F7.5,3X,F6.1,3X,F5.1,3X,F5.1,3X,F6.1,  
 16900 25 FORMAT(' B BUOYT BUOYM RAT D GR GRM PR  
 17000 1 SC HC HD N1 CON RAD EVAP')  
 17100  
 17200  
 17300 C STOP  
 17400 END  
 17500  
 17600  
 17700  
 17800  
 17900  
 18000 C SUBROUTINE AVEG(M,N)  
 18100 COMMON/AV/RHO(90),XMU(90),XK(90),P(90),HFG(90),T(90)  
 18200 COMMON/BV/AVRHO,AVMU,AVK  
 18300 AVRHO = (RHO(M) + RHO(N))/2.0  
 18400 AVMU = (XMU(M) + XMU(N))/2.0  
 18500 AVK = (XK(M) + XK(N))/2.0  
 18600  
 18700 C TYPE 1  
 18800 RETURN  
 18900 1 FORMAT(' OUT')  
 19000 END

A 70577

ME-1981-M-SIN-FAB